

Robust Deep Reinforcement Learning against Adversarial Perturbations on State Observations

Huan Zhang^{*,1} Hongge Chen^{*,2} Chaowei Xiao³
 Bo Li⁴ Mingyan Liu³ Duane Boning² Cho-Jui Hsieh¹

¹UCLA ² MIT ³University of Michigan ⁴UIUC

huan@huan-zhang.com, chenhg@mit.edu, xiaocw@umich.edu

lbo@illinois.edu, mingyan@umich.edu, boning@mtl.mit.edu, chohsieh@cs.ucla.edu

^{*}Huan Zhang and Hongge Chen contributed equally.

June 30, 2020
 (version v2; initially released on March 19, 2020)

Abstract

A deep reinforcement learning (DRL) agent observes its states through observations, which may contain natural measurement errors or adversarial noises. Since the observations deviate from the true states, they can mislead the agent into making suboptimal actions. Several works have shown this vulnerability via adversarial attacks, but how to improve the robustness of DRL under this setting has not been well studied. We show that naively applying existing techniques on improving robustness for classification tasks, like adversarial training, are ineffective for many RL tasks. We propose the state-adversarial Markov decision process (SA-MDP) to study the fundamental properties of this problem, and develop a theoretically principled policy regularization which can be applied to a large family of DRL algorithms, including proximal policy optimization (PPO), deep deterministic policy gradient (DDPG) and deep Q networks (DQN), for both discrete and continuous action control problems. We significantly improve the robustness of PPO, DDPG and DQN agents under a suite of strong white box adversarial attacks, including new attacks of our own. Additionally, we find that a robust policy noticeably improves DRL performance even without an adversary in a number of environments.

1 Introduction

With deep neural networks (DNNs) as powerful function approximators, deep reinforcement learning (DRL) has achieved great success on many complex tasks [39, 29, 27, 56, 16] and even on some safety-critical applications (e.g., autonomous driving [64, 49, 42]). Despite achieving super-human level performance on many tasks, the existence of adversarial examples [59] in DNNs and many successful attacks to DRL [21, 2, 30, 43, 70] motivates us to study robust DRL algorithms.

When an RL agent obtains its current state via observations, the observations may contain uncertainty that naturally originates from unavoidable sensor errors or equipment inaccuracy. A policy not robust to such uncertainty can lead to catastrophic failures (Figure 1). To ensure safety under the *worst case* uncertainty, in our paper we consider the adversarial setting where the observation is adversarially perturbed from s to $\nu(s)$, yet the underlying true environment state s where the agent locates is unchanged. This setting is aligned with many adversarial attacks on state observations (e.g., [21, 30]). To improve robustness under this setting, a natural approach is to extend existing adversarial defenses for supervised learning, e.g., adversarial training [26, 33, 76] to DRL. Specifically, we can attack the agent and generate trajectories adversarially during training time, and apply any existing DRL

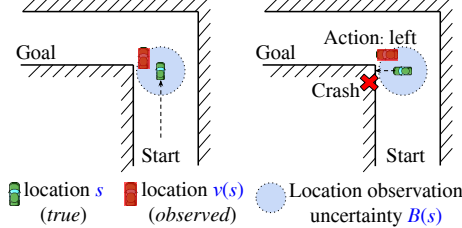


Figure 1: A car observes its location through sensors (e.g., GPS) and plans its route to the goal. Without considering the uncertainty in observed location (e.g., error of GPS coordinates), an unsafe policy may crash into the wall because the observed location and true location differ.

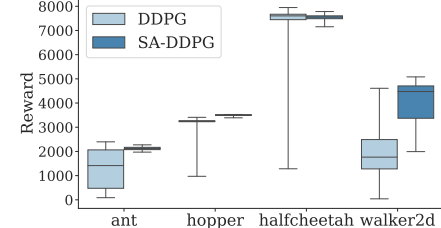


Figure 2: Box plots of rewards over 100 episodes on four Mujoco environments. Even in natural environments *without an adversary*, the *minimum rewards* DDPG agents receive can be much lower than the median. Our robust SA-DDPG agents obtain much better worst case performance.

algorithm to hopefully obtain a robust policy. Unfortunately, we show that for most environments, naive adversarial training can make training unstable and deteriorate agent performance (a similar observation is made in [3, 11]), or does not significantly improve robustness under strong attacks. Since RL and supervised learning are quite different problems, naively applying techniques from supervised learning to RL without a proper theoretical justification can be unsuccessful.

Additionally, DRL agents can be brittle even without any adversarial attacks – an agent may fail occasionally but catastrophically during regular (non-adversarial) rollouts, and debugging these failure cases can be quite challenging [62]. In Figure 2 we show a few DDPG agents achieving high median rewards. However, during 100 episodes (each episode is randomly initialized with a small noise added in OpenAI Gym) we observe occasional low reward runs. In practical applications, such a small noise can be naturally prevalent and thus prohibits the use of DRL in safety critical domains like autonomous driving. The agents trained using our proposed robust policy optimization objective (SA-DDPG) can obtain significantly better worst case reward with much less variance. To summarize, our paper studies the theory and practice of robust RL against perturbations on state observations:

- We formulate the perturbation on state observations as a modified Markov decision process (MDP), which we call state-adversarial MDP (SA-MDP), and study its fundamental properties. We show that under an optimal adversary, a stationary and Markov optimal policy may not exist for SA-MDP.
- Based on our theory of SA-MDP, we propose a theoretically principled robust policy regularizer which is related to the total variation distance or KL-divergence on perturbed policies. It can be practically and efficiently applied to a wide range of RL algorithms, including PPO, DDPG and DQN.
- We conduct experiments on 11 environments ranging from Atari games with discrete actions to complex robotic control tasks in continuous action space. Our proposed method significantly improves robustness under strong white-box attacks on state observations, including two new attacks we design, the robust SARSA attack (RS attack) and maximal action difference attack (MAD attack).

2 Related Work

Robust Reinforcement Learning Since each element of RL (observations, actions, transition dynamics and rewards) can contain uncertainty, robust RL has been studied from different perspectives. Robust Markov decision process (RMDP) [23, 40] considers the worst case perturbation from transition probabilities, and has been extended to distributional settings [71] and partially observed MDPs [41]. The agent observes the original true state from the environment and acts accordingly, but the environment can choose from a set of transition probabilities that minimizes rewards. RMDP theory has inspired robust deep Q-learning [55] and policy gradient algorithms [35, 8, 36] that are robust against small *environment changes* (e.g., changes in physical parameters like mass and length).

Several works [44, 28] consider the adversarial setting of multi-agent reinforcement learning [60, 5]. In the simplest two-player setting (referred to as minimax games in [31]), each agent chooses an action at each step, and the environment transits based on both actions. The regular Q function $Q(s, a)$ can be extended to $Q(S, a, o)$ where o is the opponent’s action and Q -learning is still convergent. This setting can be extended to deep Q learning and policy gradient algorithms [28, 44]. Pinto et al. [44] show that learning an opponent agent simultaneously can improve the agent’s performance as well as its robustness against environment turbulence and test conditions (e.g., change in mass or friction). Gu et al. [17] carried out real-world experiments on the two-player adversarial learning game. Additionally, Tessler et al. [61] considered adversarial perturbations on the action space. Fu et al. [12] investigated how to learn a robust reward. All these settings are different from ours, as we only manipulate the observations but do not change the underlying environment or actions directly.

Adversarial Attacks on State Observations in DRL Huang et al. [21] evaluate the robustness of deep reinforcement learning policies through an FGSM based attack on Atari games with discrete actions. Kos & Song [25] proposed to use the value function to guide adversarial perturbation search. Lin et al. [30] considered a more complicated case where the adversary is allowed to only attack at a subset of time steps, and used a generative model to generate attack plans luring the agent to a designated target state. Behzadan & Munir [2] studied black-box attacks on DQN with discrete action space via transferability of adversarial examples. Pattanaik et al. [43] further enhanced attacks with multi-step gradient descent and better engineered loss functions. We refer the reader to recent surveys [70, 22] for a taxonomy and a comprehensive list of adversarial attacks in DRL.

Improving Robustness for State Observations in DRL For discrete action RL tasks, Kos & Song [25] first presented preliminary results of adversarial training on Pong (one of the simplest Atari environments) using weak FGSM attacks on pixel space. Behzadan & Munir [3] applied adversarial training to several Atari games with DQN, and found it challenging for the agent to adapt to the attacks during training time – one must attack only a portion of frames, and even then the agent performance still suffers under test time attacks. For Pong, adversarial training can improve reward under attack from -21 (lowest) to -5 , yet is still far away from the optimal reward ($+21$). To obtain better performance, Mirman et al. [37], Fischer et al. [11] treat the *discrete action* outputs of DQN as labels, and apply existing certified defense for classification [38] to robustly predict actions using imitation learning. This approach outperforms [3], but it is unclear how to apply it to environments with continuous action spaces. For continuous action RL tasks (e.g., Mujoco environments), Mandlekar et al. [34] used a weak FGSM based attack with policy gradient to adversarially train a few simple RL tasks. Pattanaik et al. [43] used stronger multi-step gradient based attacks; however, their evaluation focused on robustness against environment changes rather than state perturbations. We show that *adversarial training does not reliably improve test time performance* under strong attacks in Section 4. Other related works include [19], which proposed a meta online learning procedure with a master agent detecting the presence of the adversary and switching between a few sub-policies, but did not discuss how to train a single agent robustly. [7] applied adversarial training specifically for RL-based path-finding algorithms. Lütjens et al. [32] considered the worst-case scenario during rollouts for an existing DQN agents to ensure safety, but it relies on an existing policy and does not include a training procedure. Robust DRL for perturbations on state observations, especially for continuous action space tasks, is largely unsolved and existing approaches lack proper theoretical justifications.

3 Methodology

3.1 State-Adversarial Markov Decision Process

A Markov decision process (MDP) is defined as a 4-tuple, $(\mathcal{S}, \mathcal{A}, R, p)$, where \mathcal{S} is the state space, \mathcal{A} is the action space, $R : \mathcal{S} \times \mathcal{A} \times \mathcal{S} \rightarrow \mathbb{R}$ is the reward function, and $p : \mathcal{S} \times \mathcal{A} \rightarrow \mathcal{P}(\mathcal{S})$ represents the transition probability of environment, where $\mathcal{P}(\mathcal{S})$ defines the set of all possible probability measures

on \mathcal{S} . The transition probability is $p(s'|s, a) = \Pr(s_{t+1} = s' | s_t = s, a_t = a)$, where t is the time step. We denote a stationary policy as $\pi : \mathcal{S} \rightarrow \mathcal{P}(\mathcal{A})$, the set of all stochastic and Markovian policies as Π_{MR} , the set of all deterministic and Markovian policies as Π_{MD} , and the discount factor as $0 < \gamma < 1$.

In state-adversarial MDP (SA-MDP), we introduce an adversary $\nu(s) : \mathcal{S} \rightarrow \mathcal{S}$. The adversary only perturbs the observation of the agent, such that the action is taken as $\pi(a|\nu(s))$, but the environment still transits from state s rather than $\nu(s)$ to the next state. Since $\nu(s)$ can be different from s , the agent's action from $\pi(a|\nu(s))$ may be sub-optimal, and thus the adversary is able to reduce the reward. In a real world RL problem, the adversary can be reflected as the worst case noise in measurement or state estimation uncertainty. Note that this scenario is different from the two-player Markov game [31] where both players interact with the environment directly and the opponent can change the state of the game.

To allow a formal analysis, we make the following assumptions for the adversary ν :

Assumption 1 (Stationary, Deterministic and Markovian Adversary). $\nu(s)$ is a deterministic function $\nu : \mathcal{S} \rightarrow \mathcal{S}$ which only depends on the current state s , and ν does not change over time.

This assumption holds for many adversarial attacks [21, 30, 25, 43]. These attacks only depend on the current state input and the policy or Q network so they are Markovian; the network parameters are frozen at test time, so given the same s the adversary will generate the same (stationary) perturbation. We leave the formal analysis of non-Markovian, non-stationary adversaries as future work.

Assumption 2 (Bounded Adversary Power). $\nu(s) \in B(s)$ where $B(s)$ is a set of states and $s \in B(s)$.

Assumption 2 restricts the adversary to perturb a state s only to a predefined set of states $B(s)$. $B(s)$ is usually a set of task-specific “neighbouring” states of s (e.g., bounded sensor measurement errors), which makes the observation still meaningful (yet not accurate) even with perturbations.

The definitions of adversarial value and action-value functions under ν is similar to those of regular MDP:

$$\tilde{V}_\nu^\pi(s) = \mathbb{E}_{\pi \circ \nu} \left[\sum_{k=0}^{\infty} \gamma^k r_{t+k+1} | s_t = s \right], \quad \tilde{Q}_\nu^\pi(s, a) = \mathbb{E}_{\pi \circ \nu} \left[\sum_{k=0}^{\infty} \gamma^k r_{t+k+1} | s_t = s, a_t = a \right],$$

where the reward at step- t is defined as r_t and $\pi \circ \nu$ denotes the policy under observation perturbations: $\pi(a|\nu(s))$. Based on these two assumptions, we state our theorems for the state-adversarial Markov decision process. The proofs of our theorems are provided in Appendix B.

Theorem 1 (Bellman equations for fixed π and ν). *Given $\pi : \mathcal{S} \rightarrow \mathcal{P}(\mathcal{A})$ and $\nu : \mathcal{S} \rightarrow \mathcal{S}$, we have*

$$\begin{aligned} \tilde{V}_\nu^\pi(s) &= \sum_{a \in \mathcal{A}} \pi(a|\nu(s)) \sum_{s' \in \mathcal{S}} p(s'|s, a) \left[R(s, a, s') + \gamma \tilde{V}_\nu^\pi(s') \right] \\ \tilde{Q}_\nu^\pi(s, a) &= \sum_{s' \in \mathcal{S}} p(s'|s, a) \left[R(s, a, s') + \gamma \sum_{a' \in \mathcal{A}} \pi(a'|\nu(s')) \tilde{Q}_\nu^\pi(s', a') \right]. \end{aligned}$$

We first consider the optimal adversary $\nu^*(\pi)$ that minimizes the total expected reward for a given π , and define the optimal adversarial value and action-value functions:

$$\tilde{V}_{\nu^*}^\pi(s) = \min_{\nu} \tilde{V}_\nu^\pi(s), \quad \tilde{Q}_{\nu^*}^\pi(s, a) = \min_{\nu} \tilde{Q}_\nu^\pi(s, a).$$

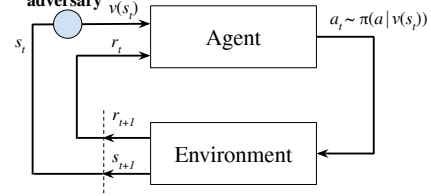


Figure 3: Reinforcement learning with perturbed state observations. The agent observes a perturbed state $\nu(s_t)$ rather than the true environment state s_t .

Theorem 2 (Bellman contraction for optimal adversary). Define Bellman operator $\mathcal{L} : \mathbb{R}^{|\mathcal{S}|} \rightarrow \mathbb{R}^{|\mathcal{S}|}$,

$$(\mathcal{L}\tilde{V}^\pi)(s) = \min_{s_\nu \in B(s)} \sum_{a \in \mathcal{A}} \pi(a|s_\nu) \sum_{s' \in \mathcal{S}} p(s'|s, a) \left[R(s, a, s') + \gamma \tilde{V}^\pi(s') \right]. \quad (1)$$

The Bellman equation for optimal adversary ν^* can be written as: $\tilde{V}_{\nu^*}^\pi = \mathcal{L}\tilde{V}_{\nu^*}^\pi$. Additionally, \mathcal{L} is a contraction that converges to $\tilde{V}_{\nu^*}^\pi$.

Based on Theorem 2 we have a policy evaluation algorithm for SA-MDP (Algorithm 1 in Appendix B), that computes $V_{\nu^*}^\pi(s)$ for each $s \in \mathcal{S}$. Given π , value functions for MDP and SA-MDP can be vastly different; Appendix A includes an example where its optimal MDP policy has 0 reward in SA-MDP.

Following the known results in MDP, we hope to find an *optimal* policy π^* for SA-MDP such that

$$\tilde{V}_{\nu^*(\pi^*)}^{\pi^*}(s) \geq \tilde{V}_{\nu^*(\pi)}^\pi(s) \quad \text{for } \forall s \in \mathcal{S} \text{ and } \forall \pi. \quad (2)$$

where the subscript $\nu^*(\pi)$ explicitly indicates that ν^* is the optimal adversary for π . Unfortunately, we show the following surprising negative results in Theorem 3 and Theorem 4:

Theorem 3. *There exists an SA-MDP and some stochastic policy $\pi \in \Pi_{MR}$ such that we cannot find a better deterministic policy $\pi' \in \Pi_{MD}$ satisfying $\tilde{V}_{\nu^*(\pi')}^{\pi'}(s) \geq \tilde{V}_{\nu^*(\pi)}^\pi(s)$ for all $s \in \mathcal{S}$.*

Contrarily, in classical MDP, for any stochastic policy we can find a deterministic policy that is at least as good as the stochastic one. With an optimal adversary in SA-MDP, it does not hold anymore.

Theorem 4. *Under the optimal ν^* , an optimal policy $\pi^* \in \Pi_{MR}$ does not always exist for SA-MDP.*

The optimal policy π^* requires to have $\tilde{V}_{\nu^*(\pi^*)}^{\pi^*}(s) \geq \tilde{V}_{\nu^*(\pi)}^\pi(s)$ for all s and any π . In an SA-MDP, surprisingly, sometimes we have to make a trade-off between the value of two states and there is no policy that can maximize the values of all states simultaneously (see Appendix A). However, not all hopes are lost and we show that under certain assumptions, the loss in performance can be bounded:

Theorem 5. *Given a policy π for a non-adversarial MDP. Under the optimal adversary ν in SA-MDP, for all $s \in \mathcal{S}$ we have*

$$\max_{s \in \mathcal{S}} \{ V^\pi(s) - \tilde{V}_{\nu^*}^{\pi^*}(s) \} \leq \alpha \max_{s \in \mathcal{S}} \max_{\hat{s} \in B(s)} D_{TV}(\pi(\cdot|s), \pi(\cdot|\hat{s})) \quad (3)$$

where $D_{TV}(\pi(\cdot|s), \pi(\cdot|\hat{s}))$ is the total variation distance between $\pi(\cdot|s)$ and $\pi(\cdot|\hat{s})$, and $\alpha := 2[1 + \frac{\gamma}{(1-\gamma)^2}] \max_{(s,a,s') \in \mathcal{S} \times \mathcal{A} \times \mathcal{S}} |R(s, a, s')|$ is a constant that does not depend on π .

Theorem 5 shows that as long as $D_{TV}(\pi(a|s), \pi(a|\hat{s}))$ is not too large for any $\hat{s} \in B(s)$ (within the power of adversary), the performance gap between $\tilde{V}_{\nu^*}^{\pi^*}(s)$ (SA-MDP) and $V^\pi(s)$ (regular MDP) can be bounded. This motivates us to regularize $D_{TV}(\pi(\cdot|s), \pi(\cdot|\hat{s}))$ during training to obtain a policy that is robust under strong adversaries. We now study a few practical DRL algorithms below.

3.2 State-Adversarial DRL for Stochastic Policies: A Case Study on PPO

We start with the most general case where the policy $\pi(a|s)$ is stochastic (e.g., in PPO [52]). The total variation distance is not easy to compute for most distributions, so we upper bound it again by KL divergence: $D_{TV}(\pi(a|s), \pi(a|\hat{s})) \leq (D_{KL}(\pi(a|s) \parallel \pi(a|\hat{s})))^2$. When Gaussian policies are used, we denote $\pi(a|s) \sim \mathcal{N}(\mu_s, \Sigma_s)$ and $\pi(a|\hat{s}) \sim \mathcal{N}(\mu_{\hat{s}}, \Sigma_{\hat{s}})$. Their KL-divergence can be given as:

$$D_{KL}(\pi(a|s) \parallel \pi(a|\hat{s})) = \frac{1}{2} (\log |\Sigma_{\hat{s}} \Sigma_s^{-1}| + \text{tr}(\Sigma_{\hat{s}}^{-1} \Sigma_s) + (\mu_{\hat{s}} - \mu_s)^\top \Sigma_{\hat{s}}^{-1} (\mu_{\hat{s}} - \mu_s) - |\mathcal{A}|). \quad (4)$$

Regularizing KL distance (4) for all $\hat{s} \in B(s)$ will lead to a smaller upper bound in (3), which is directly related to agent performance under optimal adversary. In PPO, the mean terms $\mu_s, \mu_{\hat{s}}$ are

produced by neural networks: $\mu_{\theta_\mu}(s)$ and $\mu_{\theta_\mu}(\hat{s})$, and Σ is a diagonal matrix independent of state s (i.e., $\Sigma_{\hat{s}} = \Sigma_s = \Sigma$), so regularizing the above KL-divergence over all s from sampled trajectories and all $\hat{s} \in B(s)$ leads to the following robust policy regularizer for PPO, ignoring constant terms:

$$\mathcal{R}_{\text{PPO}}(\theta_\mu) = \frac{1}{2} \sum_s \max_{\hat{s} \in B(s)} (\mu_{\theta_\mu}(\hat{s}) - \mu_{\theta_\mu}(s))^\top \Sigma^{-1} (\mu_{\theta_\mu}(\hat{s}) - \mu_{\theta_\mu}(s)) := \frac{1}{2} \sum_s \max_{\hat{s} \in B(s)} \mathcal{R}_s(\hat{s}, \theta_\mu). \quad (5)$$

We replace $\max_{s \in \mathcal{S}}$ term in (3) with a more practical and optimizer-friendly summation over all states in sampled trajectory. A similar treatment was used in TRPO [27] which was also derived as a KL-based regularizer, albeit on θ_μ space rather than on state space. However, minimizing (5) is challenging as it is a minimax objective, and we also have $\nabla_{\hat{s}} \mathcal{R}(\hat{s}, \theta_\mu)|_{\hat{s}=s} = 0$ so using gradient descent directly cannot solve the inner maximization problem to a local maximum. Instead of using the more expensive second order methods, we propose the following two approaches to solve (5).

Solving the robust policy regularizer using SGLD. Stochastic gradient Langevin dynamics (SGLD) [14] can escape saddle points and shallow local optima in non-convex optimization problems [47, 78, 6, 73], and can be used to solve the inner maximization with zero gradient at $\hat{s} = s$. SGLD uses the following update rule to find \hat{s}^K to maximize $\mathcal{R}_s(\hat{s}, \theta_\mu)$:

$$\hat{s}^{k+1} \leftarrow \text{proj} \left(\hat{s}^k - \eta_k \nabla_{\hat{s}^k} \mathcal{R}_s(\hat{s}^k, \theta_\mu) + \sqrt{2\eta_k/\beta_k} \xi \right), \quad \hat{s}^1 = s, \quad k = 1, \dots, K$$

where η_k is step size, ξ is an i.i.d. standard Gaussian random variable in $\mathbb{R}^{|\mathcal{S}|}$, β_k is an inverse temperature hyperparameter, and $\text{proj}(\cdot)$ projects the update back into $B(s)$. We find that SGLD is sufficient to escape the stationary point at $\hat{s} = s$. However, due to the non-convexity of $\mu_{\theta_\mu}(\hat{s}, \theta_\mu)$, this approach only provides a lower bound $\mathcal{R}_s(\hat{s}^K, \theta_\mu)$ of $\max_{\hat{s} \in B(s)} \mathcal{R}_s(\hat{s}, \theta_\mu)$. Minimizing this lower bound does not guarantee to minimize (5), as the gap between $\max_{\hat{s} \in B(s)} \mathcal{R}_s(\hat{s}, \theta_\mu)$ and $\mathcal{R}_s(\hat{s}^K, \theta_\mu)$ can be large.

Solving the robust policy regularizer using convex relaxations. Convex relaxation of non-linear units in neuron networks enables an efficient analysis of the outer bounds for a neural network [68, 75, 57, 9, 67, 66, 50, 58] (more background given in Appendix D). Several works have used it for certified adversarial defenses [69, 38, 65, 77], but here we use it as a generic optimization tool for solving minimax functions involving neural networks. Using this technique, we can obtain an upper bound for $\mathcal{R}_s(\hat{s}, \theta_\mu)$: $\bar{\mathcal{R}}_s(\theta_\mu) \geq \mathcal{R}_s(\hat{s}, \theta_\mu)$ for all $\hat{s} \in B(s)$. $\bar{\mathcal{R}}_s(\theta_\mu)$ is also a function of θ_μ and can be efficiently computed and optimized. We can then solve the following minimization problem:

$$\min_{\theta_\mu} \frac{1}{2} \sum_s \bar{\mathcal{R}}_s(\theta_\mu) \geq \min_{\theta_\mu} \frac{1}{2} \sum_s \max_{\hat{s} \in B(s)} \mathcal{R}_s(\hat{s}, \theta_\mu) = \min_{\theta_\mu} \mathcal{R}_{\text{PPO}}(\theta_\mu).$$

Since we minimize an *upper bound* of the inner max, the original objective (5) is guaranteed to be minimized. Using convex relaxations can also provide certain *robustness certificates* for DRL as a bonus (e.g., we can guarantee an action has bounded changes under bounded perturbations), discussed in Appendix E. We use `auto_LiRPA`, an efficient and automatic tool [72], to give $\bar{\mathcal{R}}_s(\theta_\mu)$.

Once the inner maximization problem is solved, we can add \mathcal{R}_{PPO} as part of the policy optimization objective, and solve PPO using SGD as usual. We show our full SA-PPO algorithm in Appendix F.

3.3 State-Adversarial DRL for Deterministic Policies: A Case Study on DDPG

DDPG learns a deterministic policy $\pi(s) \in \mathbb{R}^{|\mathcal{A}|}$, and in this situation, the total variation distance $D_{TV}(\pi(\cdot|s), \pi(\cdot|\hat{s}))$ is malformed, as the densities at different states s and \hat{s} are very likely to be completely non-overlapping. To address this issue, we define a smoothed version of policy, $\bar{\pi}(a|s)$ in DDPG, where we add independent Gaussian noise with variance σ^2 to each action: $\bar{\pi}(a|s) \sim \mathcal{N}(\pi(s), \sigma^2 I_{|\mathcal{A}|})$. Then we can compute $D_{TV}(\bar{\pi}(\cdot|s), \bar{\pi}(\cdot|\hat{s}))$ using the following theorem:

Theorem 6. $D_{TV}(\bar{\pi}(\cdot|s), \bar{\pi}(\cdot|\hat{s})) = \sqrt{2/\pi} \frac{d}{\sigma} + O(d^3)$, where $d = \|\pi(s) - \pi(\hat{s})\|_2$.

Thus, as long as we can penalize $\sqrt{2/\pi} \frac{d}{\sigma}$, the total variation distance between the two smoothed distributions can be bounded. In DDPG, we parameterize the policy as a policy network π_{θ_π} . Based on Theorem 5, the robust policy regularizer for DDPG is:

$$\mathcal{R}_{DDPG}(\theta_\pi) = \sqrt{2/\pi} (1/\sigma) \sum_s \max_{\hat{s} \in B(s)} \|\pi_{\theta_\pi}(s) - \pi_{\theta_\pi}(\hat{s})\|_2 \quad (6)$$

for each state s in a sampled batch of states, we need to solve a maximization problem, which can be done using SGLD or convex relaxations similarly as we have shown in Section 3.2. Note that the smoothing procedure can be done completely at test time, and during training time our goal is to keep $\max_{\hat{s} \in B(s)} \|\pi_{\theta_\pi}(s) - \pi_{\theta_\pi}(\hat{s})\|_2$ small. We show the full SA-DDPG algorithm in Appendix G.

3.4 State-Adversarial DRL for Q Learning: A Case Study on DQN

The action space for DQN is finite, and the deterministic action is determined by the max Q value: $\pi(a|s) = 1$ when $a = \arg \max_{a'} Q(s, a')$ and 0 otherwise. The total variation distance in this case is

$$D_{TV}(\pi(\cdot|s), \pi(\cdot|\hat{s})) = \begin{cases} 0 & \arg \max_a \pi(a|s) = \arg \max_a \pi(a|\hat{s}) \\ 1 & \text{otherwise.} \end{cases}$$

Thus, we want to make the top-1 action stay unchanged after perturbation, and we use a hinge-like robust policy regularizer, where $a^*(s) = \arg \max_a Q_\theta(s, a)$ and c is a small positive constant:

$$\mathcal{R}_{DQN}(\theta) := \sum_s \max \left\{ \max_{\hat{s} \in B(s)} \max_{a \neq a^*} Q_\theta(\hat{s}, a) - Q_\theta(\hat{s}, a^*(s)), -c \right\}. \quad (7)$$

The sum is over all s in a sampled batch. Unlike PPO and DDPG, it is more similar to the robustness of classification tasks, if we treat $a^*(s)$ as the “correct” label. The maximization can be solved using projected gradient descent (PGD) or convex relaxation of neural networks. Due to its similarity to classification, we defer the details on solving $\mathcal{R}_{DQN}(\theta)$ and full SA-DQN algorithm to Appendix H.

3.5 Robustness Evaluation via Adversarial Attacks under Assumption 1

In this section and Appendix C we discuss a few strong adversarial attacks under Assumption 1.

For policy gradient and actor-critic based RL algorithms, Pattanaik et al. [43] and many follow-on works use the gradient of $Q(s, a)$ to provide the direction to update states adversarially in K steps:

$$s^{k+1} = s^k - \eta \cdot \text{proj} [\nabla_{s^k} Q(s^0, \pi(s^k))], \quad k = 0, \dots, K-1, \text{ and define } \hat{s} := s^{K-1}. \quad (8)$$

Here $\text{proj}[\cdot]$ is a projection to $B(s)$, η is the learning rate, and s^0 is the state under attack. It attempts to find a state \hat{s} triggering an action $\pi(\hat{s})$ minimizing the action-value at state s^0 . The formulation in [43] has a glitch that the gradient is evaluated as $\nabla_{s^k} Q(s^k, \pi(s^k))$ rather than $\nabla_{s^k} Q(s^0, \pi(s^k))$. We found that the corrected form (8) is more successful. If Q is a perfect action-value function, \hat{s} leads to the worst action that minimizes the value at s^0 . However, this attack has a few drawbacks:

- Attack strength strongly depends on critic quality; if Q is poorly learned, is not robust against small perturbations or has obfuscated gradients, the attack fails as no correct update direction is given.
- It relies on the Q function which is specific to the training process, but not used during roll-out.
- Not applicable to many actor-critic methods (e.g., TRPO and PPO) using a learned value function $V(s)$ instead of $Q(s, a)$. Finding $\hat{s} \in B(s)$ minimizing $V(s)$ does not correctly reflect the setting of perturbing observations, as $V(\hat{s})$ represents the value of \hat{s} rather than the value of taking $\pi(\hat{s})$ at s^0 .

When we evaluate the robustness of a policy, we desire it to be independent of a specific critic network to avoid these problems. We thus propose two novel *critic independent* attacks for DDPG and PPO.

Robust SARSA (RS) attack. Since π is fixed during evaluation, we can learn its corresponding $Q^\pi(s, a)$ using on-policy temporal-difference algorithms without knowing the critic network used during training. Additionally, we find that the robustness of $Q^\pi(s, a)$ is very important; if $Q^\pi(s, a)$ is not robust against small perturbations (e.g., given a state s_0 , a small change in a will significantly reduce $Q^\pi(s_0, a)$ which does not reflect the true action-value), it cannot provide a good direction for attacks. Based on these, we use the on-policy TD-learning algorithm, SARSA [48], to learn $Q^\pi(s, a)$ (parameterized as an NN with parameters θ) with an additional robustness objective to minimize:

$$L_{RS}(\theta) = \sum_{i \in [N]} [r_i + \gamma Q_{RS}^\pi(s'_i, a'_i) - Q_{RS}^\pi(s_i, a_i)]^2 + \lambda_{RS} \sum_{i \in [N]} \max_{\hat{a} \in B(a_i)} (Q_{RS}^\pi(s_i, \hat{a}) - Q_{RS}^\pi(s_i, a_i))^2.$$

N is the batch size and each batch contains N tuples of transitions (s, a, r, s', a') sampled from agent rollouts. The first summation is the TD-loss and the second summation is the robustness penalty with regularization λ_{RS} . $B(a_i)$ is a small set near action a_i (e.g., a ℓ_∞ ball of norm 0.05 when action is normalized between 0 to 1). The inner maximization can be solved using convex relaxation of neural networks as we have done in Section 3.3. Then, we use $Q_{\theta_{RS}}^\pi$ to perform critic-based attacks as in (8). This attack sometimes significantly outperforms the attack using the critic trained along with the policy network, as its attack strength does not depend on the quality of an existing critic. We give the detailed procedure for RS attack and show the importance of the robust objective in appendix C.

Maximal Action Difference (MAD) attack. We propose another simple yet very effective attack which does not depend on a critic. Following our Theorem 5 and 6, we can find an adversarial state \hat{s} by maximizing $D_{KL}(\pi(\cdot|s) \parallel \pi(\cdot|\hat{s}))$. For actions parameterized by Gaussian mean $\pi_{\theta_\pi}(s)$ and covariance matrix Σ (independent of s), we minimize $L_{MAD}(\hat{s}) := -D_{KL}(\pi(\cdot|s) \parallel \pi(\cdot|\hat{s}))$ to find \hat{s} :

$$\arg \min_{\hat{s} \in B(s)} L_{MAD}(\hat{s}) = \arg \max_{\hat{s} \in B(s)} D_{KL}(\pi(\cdot|s) \parallel \pi(\cdot|\hat{s})) = \arg \max_{\hat{s} \in B(s)} (\pi_{\theta_\pi}(s) - \pi_{\theta_\pi}(\hat{s}))^\top \Sigma^{-1} (\pi_{\theta_\pi}(s) - \pi_{\theta_\pi}(\hat{s}))$$

For DDPG we can simply set $\Sigma = I$. The objective can be optimized using SGLD to find a good \hat{s} .

4 Experiments

In our experiments, the set of adversarial states $B(s)$ is defined as an ℓ_∞ norm ball around s with a radius ϵ : $B(s) := \{\hat{s} : \|\hat{s} - s\|_\infty \leq \epsilon\}$. Here ϵ is also referred to as the perturbation budget. In some environments, the ℓ_∞ norm is applied on normalized state representations. Our reference implementation for SA-PPO, SA-DDPG and SA-DQN is available at <https://github.com/chenhongge/StateAdvDRL>.

Evaluation of SA-PPO We use the PPO implementation from [10], which conducted hyperparameter search and published the optimal hyperparameters for PPO on three Mujoco environments in OpenAI Gym [4]. We use their optimal hyperparameters for PPO, and the same set of hyperparameters for SA-PPO without further tuning. We run Walker2d and Hopper 2×10^6 steps and Humanoid 1×10^7 steps to ensure convergence. Our PPO baselines achieve similar or better performance than reported in the literature [10, 20, 18]. Detailed hyperparameters are in Appendix F. SA-PPO has one additional regularization parameter, κ_{PPO} , for the regularizer \mathcal{R}_{PPO} , which is chosen in $\{0.01, 0.03, 0.1, 0.3, 1.0\}$. The perturbation ϵ is added into the normalized state space as ℓ_∞ noise. We include three baselines: vanilla PPO, and adversarially trained PPO [34, 43] with 50% and 100% training steps under critic attack [43]. The attack has to be conducted on $V(s)$ instead of $Q(s, a)$, as PPO does not learn a Q function during learning. We report SA-PPO objective solved using both SGLD and convex relaxation methods. We use five attacks detailed in Sec. 3.5 and Appendix C. In Table 1, we observe that *adversarial training deteriorates performance* and does not reliably improve robustness in all three environments. Our *RS attack and MAD attacks are very effective* in all environments and achieve significantly lower rewards than critic and random attacks; this shows the importance of evaluation using strong attacks. SA-PPO, solved either by SGLD or the convex relaxation objective, *significantly improves robustness* against strong attacks. Additionally, SA-PPO

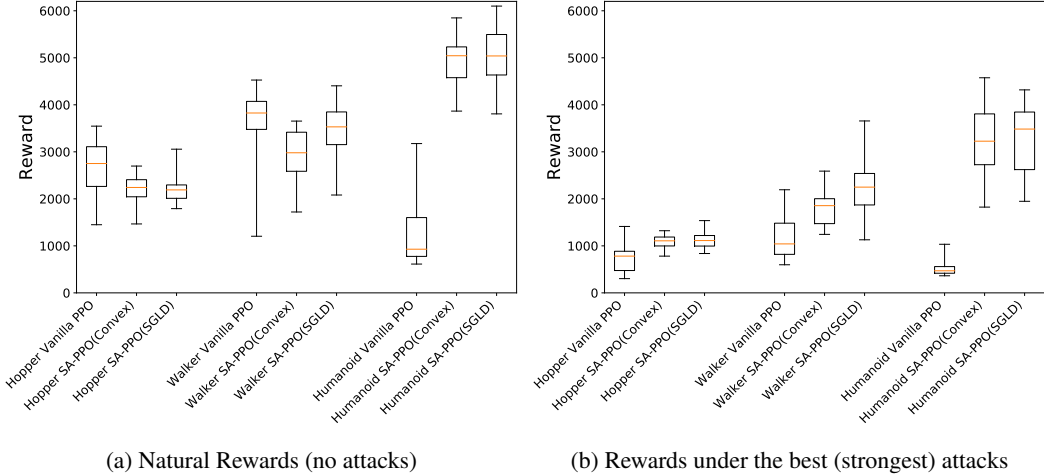


Figure 4: Box plots of natural and attack rewards for PPO and SA-PPO (solved by SGLD or convex relaxations) on 3 environments. Each box is obtained from **30 models** trained with the same parameters as in models reported in Table 1 and tested for 50 episodes. The red lines inside the boxes are median rewards, and the upper and lower sides of the boxes show 25% and 75% percentile rewards of 30 models. The line segments outside of the boxes show min or max rewards.

achieves natural performance (without attacks) similar to that of vanilla PPO in Walker2d and Hopper, and *significantly improves the reward in Humanoid environment*. Humanoid has high state-space dimension (376) and is usually hard to train [18], and our results suggest that a robust objective can be helpful even in a non-adversarial setting. We include more results in Appendix I.

Table 1: Average rewards \pm standard deviation over 50 episodes on three baselines and SA-PPO. We report natural rewards (no attacks) and rewards under five adversarial attacks. In each row we bold the best (lowest) attack reward over all five attacks. The gray rows are the most robust models.

Env.	ℓ_∞ norm perturbation budget ϵ	Method	Natural Reward	Attack Reward				Best Attack
				Critic	Random	MAD	RS	
Hopper	0.075	PPO (vanilla)	2554 \pm 853	1464 \pm 523	2101 \pm 793	1410 \pm 655	794 \pm 238	781\pm175
		PPO (adv. 50%)	174 \pm 146	69 \pm 83	141 \pm 128	42\pm 46	49 \pm 50	44 \pm 43
		PPO (adv. 100%)	6.1 \pm 2.6	4.4 \pm 1.8	6.1 \pm 3.2	5.8 \pm 2.7	3.8 \pm 0.9	3.6\pm 0.5
		SA-PPO (SGLD)	2278\pm 957	3239\pm 808	2155\pm 904	2178 \pm 878	1112\pm 373	1171 \pm 343
		SA-PPO (Convex)	2197 \pm 744	2996 \pm 883	2488 \pm 950	2123 \pm 827	1031\pm365	1065 \pm 378
Walker2d	0.05	PPO (vanilla)	3460 \pm 1170	3424 \pm 1295	3007 \pm 1200	2869 \pm 1271	1336 \pm 654	1307\pm 749
		PPO (adv. 50%)	-11 \pm 0.9	-10.6 \pm 0.86	-10.99 \pm 0.95	-10.78 \pm 0.89	-11.55\pm 0.79	-11.37 \pm 0.87
		PPO (adv. 100%)	-113 \pm 4.14	-111.9 \pm 4.13	-111 \pm 4.27	-112 \pm 4.08	-114.4 \pm 4.0	-114.5\pm 4.09
		SA-PPO (SGLD)	3566 \pm 1363	4076 \pm 997	3898 \pm 1133	3837 \pm 1215	2415\pm 1451	2615 \pm 1299
		SA-PPO (Convex)	3654\pm 1459	3504\pm 1529	3808\pm 1305	2966\pm 1716	2841\pm 1679	3136 \pm 1865
Humanoid	0.075	PPO (vanilla)	2229 \pm 1192	1889 \pm 938	2073 \pm 1197	1134 \pm 585	672\pm 235	784 \pm 336
		PPO (adv. 50%)	234 \pm 28	198 \pm 58	240 \pm 19.4	148 \pm 73	98\pm 69	101.5 \pm 66.4
		PPO (adv. 100%)	141.4 \pm 20.6	140.25 \pm 16.6	142.13 \pm 16	140.23 \pm 34.5	113.2 \pm 18.5	112.6\pm 13.88
		SA-PPO (SGLD)	5336 \pm 1704	5766 \pm 1414	5150 \pm 1839	5361 \pm 1773	4285\pm 2016	4369 \pm 1929
		SA-PPO (Convex)	4986 \pm 1596	5387 \pm 1436	4790 \pm 1882	4549 \pm 1919	4392\pm 2122	4700 \pm 1801

Because PPO training can have large performance variance across multiple runs, to show that our SA-PPO can consistently obtain a robust model, we repeatedly train each environment using SA-PPO and vanilla PPO **30 times** and attack all models we obtained. In Figures 4a and 4b we show the box plot of the natural and best attack reward for these PPO and SA-PPO models. We can see that the best attack reward of most SA-PPO models are consistently better than PPO models (in terms of median, 25% and 75% percentile rewards over 30 repetitions).

Evaluation of SA-DDPG We use a high quality DDPG implementation [54] as our baseline, achieving similar or better performance on five Mujoco environments as in the literature [29, 13]. For SA-DDPG, we use the same set of hyperparameters as in DDPG [54] (detailed in Appendix G), except for the additional regularization term κ_{DDPG} for $\mathcal{R}_{\text{DDPG}}$ which is searched in $\{3, 10, 30, 100, 300\}$. The ℓ_∞ perturbation ϵ is added into the normalized state space. We include vanilla DDPG, ad-

Table 2: Average rewards \pm standard deviation over 50 episodes on DDPG, adversarial training [43] (50% and 100% steps) and SA-DDPG. To avoid clutter, we only report attack rewards under the best (strongest) attack over all five attacks; full results of all 5 attacks available in Appendix I. **Bold** numbers indicate the most robust model; *italic* numbers indicate models with poor robustness.

Environment		Ant	Hopper	Inverted Pendulum	Reacher	Walker2d
ℓ_∞ norm perturbation budget ϵ		0.2	0.075	0.5	1.5	0.15
DDPG (vanilla)	Natural Reward	1633 \pm 631	3180 \pm 390	1000 \pm 0	-4.4 \pm 1.6	2247 \pm 1177
	Attack Reward (best)	<i>160 \pm 301</i>	<i>704 \pm 228</i>	<i>285 \pm 232</i>	<i>-27.85 \pm 5.83</i>	<i>711 \pm 663</i>
DDPG (adv. 50%)	Natural Reward	715 \pm 265	3010 \pm 460	1000 \pm 0	-4.79 \pm 1.49	1029 \pm 316
	Attack Reward (best)	<i>216 \pm 235</i>	<i>3.8 \pm 3.4</i>	<i>106 \pm 81</i>	<i>-32.4 \pm 6.2</i>	<i>103 \pm 118</i>
DDPG (adv. 100%)	Natural Reward	63.8 \pm 79	2680 \pm 810	1000 \pm 0	-5.97 \pm 2.39	1242 \pm 254
	Attack Reward (best)	<i>-57.5 \pm 71</i>	<i>413 \pm 552</i>	<i>345 \pm 290</i>	<i>-31.3 \pm 4.6</i>	<i>41.7 \pm 20.1</i>
SA-DDPG (SGLD)	Natural Reward	1503 \pm 502	3035 \pm 4.34	1000 \pm 0	-5.2 \pm 1.64	2760 \pm 1563
	Attack Reward (best)	1251 \pm 543	<i>2537 \pm 745</i>	<i>1000 \pm 0</i>	<i>-11.9 \pm 5.2</i>	817 \pm 747
SA-DDPG (convex relax)	Natural Reward	2111 \pm 159	3496 \pm 30.8	1000 \pm 0	-5.2 \pm 2.12	4234 \pm 854
	Attack Reward (best)	1959 \pm 105	1722 \pm 599	878 \pm 279	-13.9 \pm 3.8	1945 \pm 1143

Table 3: Average rewards \pm std and action certification rate over 50 episodes on three baselines and SA-DQN. We report natural rewards (no attacks) and PGD attack rewards (under 10-step PGD). Action Cert. Rate is the proportion of the actions during rollout that are guaranteed unchanged by any attacks within the given ϵ . **Bold** numbers indicate the most robust model; *italic* numbers indicate models with poor robustness.

Environment		Pong	Freeway	BankHeist	RoadRunner	Acrobot
ℓ_∞ norm perturbation budget ϵ		1/255				0.2
DQN (vanilla)	Natural Reward	20.7 \pm 0.5	32.9 \pm 0.7	1308.4 \pm 24.1	36946.0 \pm 6089.0	-67.5 \pm 8.8
	PGD Attack Reward	<i>-21.0 \pm 0.0</i>	<i>0.0 \pm 0.0</i>	<i>56.4 \pm 21.2</i>	<i>0.0 \pm 0.0</i>	<i>-349.7 \pm 178.0</i>
	Action Cert. Rate	0.0	0.0	0.0	0.0	0.735
DQN Adv. Training (attack 50% frames) Behzadan & Munir [3]	Natural Reward	10.1 \pm 6.6	25.4 \pm 0.8	1126.0 \pm 70.9	22944.0 \pm 6532.5	-82.8 \pm 9.9
	PGD Attack Reward	<i>-21.0 \pm 0.0</i>	<i>0.0 \pm 0.0</i>	<i>9.4 \pm 13.6</i>	<i>14.0 \pm 34.7</i>	<i>-155.1 \pm 179.6</i>
	Action Cert. Rate	0.0	0.0	0.0	0.0	0.718
Imitation learning Fischer et al. [11]	Natural Reward	19.73	32.93	238.66	12106.67	—
	PGD Attack Reward	18.13	32.53	<i>190.67</i>	5753.33	—
SA-DQN (PGD)	Natural Reward	21.0 \pm 0.0	33.9 \pm 0.4	1245.2 \pm 14.5	34032.0 \pm 3845.0	-67.5 \pm 9.0
	PGD Attack Reward	21.0 \pm 0.0	23.7 \pm 2.3	1006.0 \pm 226.4	20402.0 \pm 7551.1	-116 \pm 21.7
	Action Cert. Rate	0.0	0.0	0.0	0.0	0.707
SA-DQN (convex)	Natural Reward	21.0 \pm 0.0	30.78 \pm 0.5	1041.4 \pm 12.3	15172.0 \pm 791.7	-79.4 \pm 17.4
	PGD Attack Reward	20.1 \pm 0.0	30.36 \pm 0.7	1043.6 \pm 9.5	15280 \pm 827.7	-86.7 \pm 19.9
	Action Cert. Rate	1.000	0.995	0.997	0.969	0.856

versariably trained DDPG [43] with 50% or 100% of training steps under attack as baselines, and we evaluate SA-DDPG solved with SGLD and convex relaxations. We use the same set of five attacks, but only report the *strongest attack* (lowest reward) in Table 2 (full results in Appendix I). We observe that *adversarial training is not effective* in many environments, achieving low rewards with or without attacks. SA-DDPG *significantly improves robustness under strong attacks* in all five environments. Similar to the observations on SA-PPO, SA-DDPG can improve natural agent performance in environments (Ant and Walker2d) with relatively high dimensional state space (111 and 17). Additionally, when trained using convex relaxations, SA-DDPG has less variance during rollout (Figure 2).

To show that our SA-DDPG can consistently obtain a robust model and we do not cherry-pick good results, we repeatedly train all 5 environments using SA-DDPG and DDPG **11 times** each and attack all models. We report the median, minimum, 25% and 75% rewards of 11 models in box plots. The results are shown in Figure 5. We can observe that SA-DDPG is able to consistently improve the robustness: the median, 25% and 75% percentile rewards under attacks are significantly and consistently better than vanilla DDPG over all 5 environments.

Evaluation of SA-DQN We implement DoubleDQN [63] and Prioritized Experience Replay [51] on four Atari games and one classic control problem, Acrobot. Detailed parameters and training procedures are in Appendix H. For Atari games, we normalize the pixel values to $[0, 1]$ and we add ℓ_∞ adversarial noise with norm $\epsilon = 1/255$. For Acrobot, we normalize ϵ with element-wise standard deviation of state values collected over 100 episodes. We include vanilla DQNs and adversarially

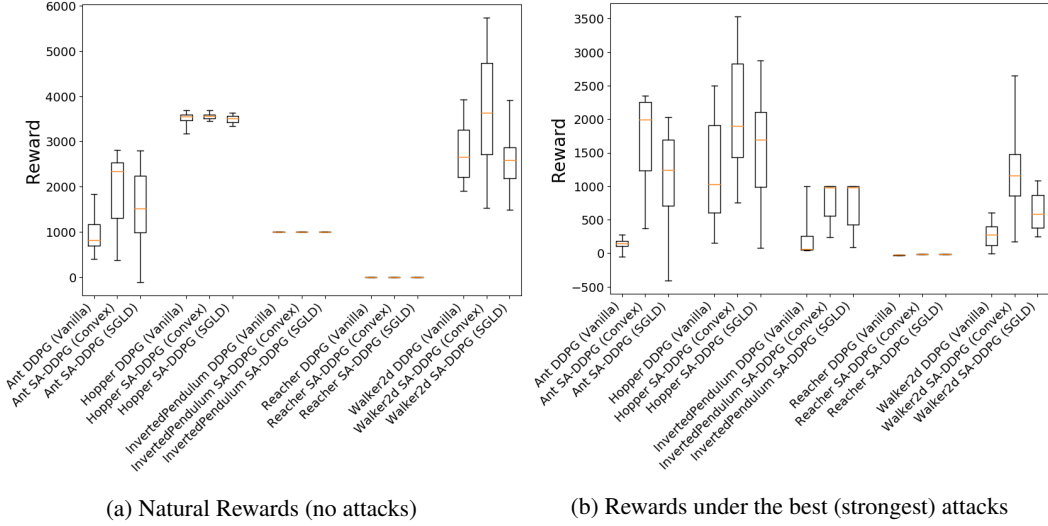


Figure 5: Box plots of natural and attack rewards for DDPG and SA-DDPG. Each box is obtained from **11 models** trained with the same parameters as the models reported in Table 2 and tested for 50 episodes (each sample of the box is an average reward over 50 episodes). The red lines inside the boxes are median rewards, and the upper and lower sides of the boxes show 25% and 75% percentile rewards. The line segments outside of the boxes show min or max rewards.

trained DQNs with 50% of frames under attack [3] during training time as baselines, and we report results of robust imitation learning based approach as in [11]. We evaluate all methods under 10-step untargeted PGD attacks (Appendix C), except that results from [11] was evaluated using a weaker four-step PGD attack. In Table 3, we see that our SA-DQN achieves much higher rewards under attacks in most environments, and naive adversarial training is mostly ineffective under strong attacks. We obtain better rewards than [11] in most environments, as we learn the agent directly rather than using two-step imitation learning.

Robustness certificates. When our robust policy regularizer is trained using convex relaxations, we can obtain certain robustness certification under observation perturbations. For SA-DQN, we can guarantee over 99.5% of actions do not change under any norm bounded perturbations for three environments (Table 3). For a simple environment like Pong, we can guarantee actions do not change for all frames during rollouts, thus guarantee the accumulative rewards under perturbation. For SA-DDPG, the *upper bounds* on the maximal ℓ_2 difference in action changes is a few times smaller than baseline for all five environments (results deferred to Appendix I).

5 Conclusions and Remarks

The field of reinforcement learning (RL) is being heavily developed in recent years, yet the robustness of RL has not been investigated as thoroughly as in the supervised learning setting. Reinforcement learning has the great potential to be applied into many mission-critical tasks such as autonomous driving [53, 49, 74], if its robustness can be established. The robustness considered in our paper is important for many realistic settings such as sensor noise, measurement errors, and man-in-the-middle (MITM) attacks for a DRL system. Our paper is the first work that studies this problem in a fundamental and systematic manner, and derives principles that are widely applicable to existing RL algorithms. We believe the theoretical framework and comprehensive experiments in our work will inform and inspire further research on robust deep reinforcement learning.

References

- [1] Achiam, J., Held, D., Tamar, A., and Abbeel, P. Constrained policy optimization. In *Proceedings of the 34th International Conference on Machine Learning-Volume 70*, pp. 22–31. JMLR. org, 2017.
- [2] Behzadan, V. and Munir, A. Vulnerability of deep reinforcement learning to policy induction attacks. In *International Conference on Machine Learning and Data Mining in Pattern Recognition*, pp. 262–275. Springer, 2017.
- [3] Behzadan, V. and Munir, A. Whatever does not kill deep reinforcement learning, makes it stronger. *arXiv preprint arXiv:1712.09344*, 2017.
- [4] Brockman, G., Cheung, V., Pettersson, L., Schneider, J., Schulman, J., Tang, J., and Zaremba, W. OpenAI Gym. *arXiv preprint arXiv:1606.01540*, 2016.
- [5] Bu, L., Babu, R., De Schutter, B., et al. A comprehensive survey of multiagent reinforcement learning. *IEEE Transactions on Systems, Man, and Cybernetics, Part C (Applications and Reviews)*, 38(2):156–172, 2008.
- [6] Bubeck, S., Eldan, R., and Lehec, J. Finite-time analysis of projected Langevin Monte Carlo. In *Advances in Neural Information Processing Systems*, pp. 1243–1251, 2015.
- [7] Chen, T., Niu, W., Xiang, Y., Bai, X., Liu, J., Han, Z., and Li, G. Gradient band-based adversarial training for generalized attack immunity of A3C path finding. *arXiv preprint arXiv:1807.06752*, 2018.
- [8] Derman, E., Mankowitz, D. J., Mann, T. A., and Mannor, S. Soft-robust actor-critic policy-gradient. *arXiv preprint arXiv:1803.04848*, 2018.
- [9] Dvijotham, K., Stanforth, R., Gowal, S., Mann, T., and Kohli, P. A dual approach to scalable verification of deep networks. *UAI*, 2018.
- [10] Engstrom, L., Ilyas, A., Santurkar, S., Tsipras, D., Janoos, F., Rudolph, L., and Madry, A. Implementation matters in deep policy gradients: A case study on PPO and TRPO. *arXiv preprint arXiv:2005.12729*, 2020.
- [11] Fischer, M., Mirman, M., and Vechev, M. Online robustness training for deep reinforcement learning. *arXiv preprint arXiv:1911.00887*, 2019.
- [12] Fu, J., Luo, K., and Levine, S. Learning robust rewards with adversarial inverse reinforcement learning. *arXiv preprint arXiv:1710.11248*, 2017.
- [13] Fujimoto, S., Van Hoof, H., and Meger, D. Addressing function approximation error in actor-critic methods. *arXiv preprint arXiv:1802.09477*, 2018.
- [14] Gelfand, S. B. and Mitter, S. K. Recursive stochastic algorithms for global optimization in \mathbb{R}^d . *SIAM Journal on Control and Optimization*, 29(5):999–1018, 1991.
- [15] Gowal, S., Dvijotham, K., Stanforth, R., Bunel, R., Qin, C., Uesato, J., Mann, T., and Kohli, P. On the effectiveness of interval bound propagation for training verifiably robust models. *arXiv preprint arXiv:1810.12715*, 2018.
- [16] Gu, S., Lillicrap, T., Sutskever, I., and Levine, S. Continuous deep Q-learning with model-based acceleration. In *International Conference on Machine Learning*, pp. 2829–2838, 2016.
- [17] Gu, Z., Jia, Z., and Choset, H. Adversary A3C for robust reinforcement learning. *arXiv preprint arXiv:1912.00330*, 2019.
- [18] Hämäläinen, P., Babadi, A., Ma, X., and Lehtinen, J. PPO-CMA: Proximal policy optimization with covariance matrix adaptation. *arXiv preprint arXiv:1810.02541*, 2018.

[19] Havens, A., Jiang, Z., and Sarkar, S. Online robust policy learning in the presence of unknown adversaries. In *Advances in Neural Information Processing Systems*, pp. 9916–9926, 2018.

[20] Henderson, P., Islam, R., Bachman, P., Pineau, J., Precup, D., and Meger, D. Deep reinforcement learning that matters. In *Thirty-Second AAAI Conference on Artificial Intelligence*, 2018.

[21] Huang, S., Papernot, N., Goodfellow, I., Duan, Y., and Abbeel, P. Adversarial attacks on neural network policies. *arXiv preprint arXiv:1702.02284*, 2017.

[22] Ilahi, I., Usama, M., Qadir, J., Janjua, M. U., Al-Fuqaha, A., Hoang, D. T., and Niyato, D. Challenges and countermeasures for adversarial attacks on deep reinforcement learning. *arXiv preprint arXiv:2001.09684*, 2020.

[23] Iyengar, G. N. Robust dynamic programming. *Mathematics of Operations Research*, 30(2):257–280, 2005.

[24] Kakade, S. and Langford, J. Approximately optimal approximate reinforcement learning. In *ICML*, volume 2, pp. 267–274, 2002.

[25] Kos, J. and Song, D. Delving into adversarial attacks on deep policies. *arXiv preprint arXiv:1705.06452*, 2017.

[26] Kurakin, A., Goodfellow, I., and Bengio, S. Adversarial machine learning at scale. *arXiv preprint arXiv:1611.01236*, 2016.

[27] Levine, S., Abbeel, P., Jordan, M., and Moritz, P. Trust region policy optimization. In *International Conference on Machine Learning*, pp. 1889–1897, 2015.

[28] Li, S., Wu, Y., Cui, X., Dong, H., Fang, F., and Russell, S. Robust multi-agent reinforcement learning via minimax deep deterministic policy gradient. In *Proceedings of the AAAI Conference on Artificial Intelligence*, volume 33, pp. 4213–4220, 2019.

[29] Lillicrap, T. P., Hunt, J. J., Pritzel, A., Heess, N., Erez, T., Tassa, Y., Silver, D., and Wierstra, D. Continuous control with deep reinforcement learning. *arXiv preprint arXiv:1509.02971*, 2015.

[30] Lin, Y.-C., Hong, Z.-W., Liao, Y.-H., Shih, M.-L., Liu, M.-Y., and Sun, M. Tactics of adversarial attack on deep reinforcement learning agents. *arXiv preprint arXiv:1703.06748*, 2017.

[31] Littman, M. L. Markov games as a framework for multi-agent reinforcement learning. In *Machine Learning Proceedings 1994*, pp. 157–163. Elsevier, 1994.

[32] Lütjens, B., Everett, M., and How, J. P. Certified adversarial robustness for deep reinforcement learning. *arXiv preprint arXiv:1910.12908*, 2019.

[33] Madry, A., Makelov, A., Schmidt, L., Tsipras, D., and Vladu, A. Towards deep learning models resistant to adversarial attacks. *ICLR*, 2018.

[34] Mandlekar, A., Zhu, Y., Garg, A., Fei-Fei, L., and Savarese, S. Adversarially robust policy learning: Active construction of physically-plausible perturbations. In *2017 IEEE/RSJ International Conference on Intelligent Robots and Systems (IROS)*, pp. 3932–3939. IEEE, 2017.

[35] Mankowitz, D. J., Mann, T. A., Bacon, P.-L., Precup, D., and Mannor, S. Learning robust options. In *Thirty-Second AAAI Conference on Artificial Intelligence*, 2018.

[36] Mankowitz, D. J., Levine, N., Jeong, R., Abdolmaleki, A., Springenberg, J. T., Mann, T., Hester, T., and Riedmiller, M. Robust reinforcement learning for continuous control with model misspecification. *arXiv preprint arXiv:1906.07516*, 2019.

[37] Mirman, M., Fischer, M., and Vechev, M. Distilled agent DQN for provable adversarial robustness, 2018. URL <https://openreview.net/forum?id=ryeAy3AqYm>.

[38] Mirman, M., Gehr, T., and Vechev, M. Differentiable abstract interpretation for provably robust neural networks. In *International Conference on Machine Learning*, pp. 3575–3583, 2018.

[39] Mnih, V., Kavukcuoglu, K., Silver, D., Rusu, A. A., Veness, J., Bellemare, M. G., Graves, A., Riedmiller, M., Fidjeland, A. K., Ostrovski, G., et al. Human-level control through deep reinforcement learning. *Nature*, 518(7540):529–533, 2015.

[40] Nilim, A. and El Ghaoui, L. Robustness in Markov decision problems with uncertain transition matrices. In *Advances in Neural Information Processing Systems*, pp. 839–846, 2004.

[41] Osogami, T. Robust partially observable Markov decision process. In *International Conference on Machine Learning*, pp. 106–115, 2015.

[42] Pan, X., You, Y., Wang, Z., and Lu, C. Virtual to real reinforcement learning for autonomous driving. *arXiv preprint arXiv:1704.03952*, 2017.

[43] Pattanaik, A., Tang, Z., Liu, S., Bommannan, G., and Chowdhary, G. Robust deep reinforcement learning with adversarial attacks. In *Proceedings of the 17th International Conference on Autonomous Agents and MultiAgent Systems*, pp. 2040–2042. International Foundation for Autonomous Agents and Multiagent Systems, 2018.

[44] Pinto, L., Davidson, J., Sukthankar, R., and Gupta, A. Robust adversarial reinforcement learning. In *Proceedings of the 34th International Conference on Machine Learning-Volume 70*, pp. 2817–2826. JMLR. org, 2017.

[45] Pirotta, M., Restelli, M., Pecorino, A., and Calandriello, D. Safe policy iteration. In *International Conference on Machine Learning*, pp. 307–315, 2013.

[46] Puterman, M. L. *Markov decision processes: discrete stochastic dynamic programming*. John Wiley & Sons, 2014.

[47] Raginsky, M., Rakhlin, A., and Telgarsky, M. Non-convex learning via stochastic gradient Langevin dynamics: a nonasymptotic analysis. *arXiv preprint arXiv:1702.03849*, 2017.

[48] Rummery, G. A. and Niranjan, M. *On-line Q-learning using connectionist systems*, volume 37. University of Cambridge, Department of Engineering Cambridge, UK, 1994.

[49] Sallab, A. E., Abdou, M., Perot, E., and Yogamani, S. Deep reinforcement learning framework for autonomous driving. *Electronic Imaging*, 2017(19):70–76, 2017.

[50] Salman, H., Yang, G., Zhang, H., Hsieh, C.-J., and Zhang, P. A convex relaxation barrier to tight robustness verification of neural networks. In *Advances in Neural Information Processing Systems 32*, pp. 9832–9842. Curran Associates, Inc., 2019.

[51] Schaul, T., Quan, J., Antonoglou, I., and Silver, D. Prioritized experience replay. *arXiv preprint arXiv:1511.05952*, 2015.

[52] Schulman, J., Wolski, F., Dhariwal, P., Radford, A., and Klimov, O. Proximal policy optimization algorithms. *arXiv preprint arXiv:1707.06347*, 2017.

[53] Shalev-Shwartz, S., Shammah, S., and Shashua, A. Safe, multi-agent, reinforcement learning for autonomous driving. *arXiv preprint arXiv:1610.03295*, 2016.

[54] Shangtong, Z. Modularized implementation of deep RL algorithms in PyTorch. <https://github.com/ShangtongZhang/DeepRL>, 2018.

[55] Shashua, S. D.-C. and Mannor, S. Deep robust Kalman filter. *arXiv preprint arXiv:1703.02310*, 2017.

[56] Silver, D., Huang, A., Maddison, C. J., Guez, A., Sifre, L., Van Den Driessche, G., Schrittwieser, J., Antonoglou, I., Panneershelvam, V., Lanctot, M., et al. Mastering the game of go with deep neural networks and tree search. *nature*, 529(7587):484, 2016.

[57] Singh, G., Gehr, T., Mirman, M., Püschel, M., and Vechev, M. Fast and effective robustness certification. In *Advances in Neural Information Processing Systems*, pp. 10825–10836, 2018.

[58] Singh, G., Gehr, T., Püschel, M., and Vechev, M. An abstract domain for certifying neural networks. *Proceedings of the ACM on Programming Languages*, 3(POPL):41, 2019.

[59] Szegedy, C., Zaremba, W., Sutskever, I., Bruna, J., Erhan, D., Goodfellow, I., and Fergus, R. Intriguing properties of neural networks. In *ICLR*, 2013.

[60] Tan, M. Multi-agent reinforcement learning: Independent vs. cooperative agents. In *Proceedings of the Tenth International Conference on Machine Learning*, pp. 330–337, 1993.

[61] Tessler, C., Efroni, Y., and Mannor, S. Action robust reinforcement learning and applications in continuous control. *arXiv preprint arXiv:1901.09184*, 2019.

[62] Uesato, J., Kumar, A., Szepesvari, C., Erez, T., Ruderman, A., Anderson, K., Heess, N., Kohli, P., et al. Rigorous agent evaluation: An adversarial approach to uncover catastrophic failures. *arXiv preprint arXiv:1812.01647*, 2018.

[63] Van Hasselt, H., Guez, A., and Silver, D. Deep reinforcement learning with double Q-learning. In *Thirtieth AAAI Conference on Artificial Intelligence*, 2016.

[64] Voyage. Introducing voyage deepdrive -unlocking the potential of deep reinforcement learning. <https://news.voyage.auto/introducing-voyage-deepdrive-69b3cf0f0be6>, 2019.

[65] Wang, S., Chen, Y., Abdou, A., and Jana, S. Mixtrain: Scalable training of formally robust neural networks. *arXiv preprint arXiv:1811.02625*, 2018.

[66] Wang, S., Pei, K., Whitehouse, J., Yang, J., and Jana, S. Efficient formal safety analysis of neural networks. In *Advances in Neural Information Processing Systems*, pp. 6367–6377, 2018.

[67] Weng, T.-W., Zhang, H., Chen, H., Song, Z., Hsieh, C.-J., Daniel, L., Boning, D., and Dhillon, I. Towards fast computation of certified robustness for ReLU networks. In *International Conference on Machine Learning*, pp. 5273–5282, 2018.

[68] Wong, E. and Kolter, Z. Provable defenses against adversarial examples via the convex outer adversarial polytope. In *International Conference on Machine Learning*, pp. 5283–5292, 2018.

[69] Wong, E., Schmidt, F., Metzen, J. H., and Kolter, J. Z. Scaling provable adversarial defenses. In *NIPS*, 2018.

[70] Xiao, C., Pan, X., He, W., Peng, J., Sun, M., Yi, J., Li, B., and Song, D. Characterizing attacks on deep reinforcement learning. *arXiv preprint arXiv:1907.09470*, 2019.

[71] Xu, H. and Mannor, S. Distributionally robust markov decision processes. In *Advances in Neural Information Processing Systems*, pp. 2505–2513, 2010.

[72] Xu, K., Shi, Z., Zhang, H., Huang, M., Chang, K.-W., Kailkhura, B., Lin, X., and Hsieh, C.-J. Automatic perturbation analysis on general computational graphs. *arXiv preprint arXiv:2002.12920*, 2020.

[73] Xu, P., Chen, J., Zou, D., and Gu, Q. Global convergence of langevin dynamics based algorithms for nonconvex optimization. In *Advances in Neural Information Processing Systems*, pp. 3122–3133, 2018.

- [74] You, C., Lu, J., Filev, D., and Tsiotras, P. Advanced planning for autonomous vehicles using reinforcement learning and deep inverse reinforcement learning. *Robotics and Autonomous Systems*, 114:1–18, 2019.
- [75] Zhang, H., Weng, T.-W., Chen, P.-Y., Hsieh, C.-J., and Daniel, L. Efficient neural network robustness certification with general activation functions. In *NIPS*, 2018.
- [76] Zhang, H., Yu, Y., Jiao, J., Xing, E. P., Ghaoui, L. E., and Jordan, M. I. Theoretically principled trade-off between robustness and accuracy. *arXiv preprint arXiv:1901.08573*, 2019.
- [77] Zhang, H., Chen, H., Xiao, C., Li, B., Boning, D., and Hsieh, C.-J. Towards stable and efficient training of verifiably robust neural networks. *ICLR*, 2020.
- [78] Zhang, Y., Liang, P., and Charikar, M. A hitting time analysis of stochastic gradient Langevin dynamics. *arXiv preprint arXiv:1702.05575*, 2017.

Summary of Appendix Results

- We provide more empirical results in Section I. To demonstrate the convergence of our algorithm, we repeat each experiment at least 10 times and plot the convergence of rewards during multiple runs. We found that for some environments (like Humanoid) we can significantly and consistently improve baseline performance. We also evaluate some settings under multiple perturbation strength ϵ .
- Readers who are interested in SA-MDP can find an example of SA-MDP in Section A and complete proofs in Section B.
- Readers who are interested in adversarial attacks can find more details about our new attacks and existing attacks in Section C. Especially, we discussed how a robust critic can help in attacking RL, and show experiments on the improvements gained by the robustness objective during attack.
- Readers who want to know more background of convex relaxations of neural networks (used in our work to solve the minimax objective) can refer to Section D.
- We provide detailed algorithm and hyperparameters for SA-PPO in Section F. We provide details for SA-DDPG in Section G. We provide details for SA-DQN in Section H.

A An example of SA-MDP

We first show a simple environment and solve it under different settings of MDP and SA-MDP. The environment have three states $\mathcal{S} = \{S_1, S_2, S_3\}$ and 2 actions $\mathcal{A} = \{A_1, A_2\}$. The transition probabilities and rewards are defined as (unmentioned probabilities and rewards are 0):

$$\begin{aligned}
\Pr(s' = S_1 | s = S_1, a = A_1) &= 1.0 \\
\Pr(s' = S_2 | s = S_1, a = A_2) &= 1.0 \\
\Pr(s' = S_2 | s = S_2, a = A_2) &= 1.0 \\
\Pr(s' = S_3 | s = S_2, a = A_1) &= 1.0 \\
\Pr(s' = S_1 | s = S_3, a = A_2) &= 1.0 \\
\Pr(s' = S_2 | s = S_3, a = A_1) &= 1.0 \\
R(s = S_1, a = A_2, s' = S_2) &= 1.0 \\
R(s = S_2, a = A_1, s' = S_2) &= 1.0 \\
R(s = S_3, a = A_1, s' = S_3) &= 1.0
\end{aligned}$$

The environment is illustrated in Figure 6. For the power of adversary, we allow ν to perturb one state to any other two neighbouring states:

$$B_\nu(S_1) = B_\nu(S_2) = B_\nu(S_3) = \{S_1, S_2, S_3\}$$

Now we evaluate various policies for MDP and SA-MDP for this environment. We use $\gamma = 0.99$ as the discount factor. A stationary and Markovian policy in this environment can be described by 3 parameters p_{11}, p_{21}, p_{31} where $p_{ij} \in [0, 1]$ denotes the probability $\Pr(a = A_j | s = S_i)$.

- **Optimal Policy for MDP.** For a regular MDP, the optimal solution is $p_{11} = 0, p_{21} = 1, p_{31} = 1$. We take A_2 to receive reward and leave S_1 , and then keep doing A_1 in S_2 and S_3 . The values for each state are $V(S_1) = V(S_2) = V(S_3) = \frac{1}{1-\gamma} = 100$, which is optimal. However, this policy obtains $V(S_1) = V(S_2) = V(S_3) = 0$ for SA-MDP, because we can set $\nu(S_1) = S_2, \nu(S_2) = S_1, \nu(S_3) = S_1$ and consequentially we always take the wrong action receiving 0 reward.

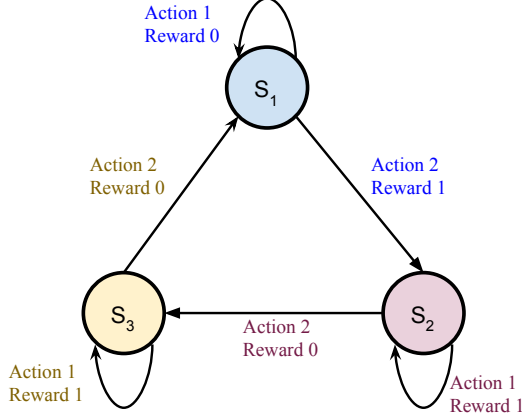


Figure 6: A simple 3-state environment.

- **A Stochastic Policy for MDP and SA-MDP.** We consider a stochastic policy where $p_{11} = p_{21} = p_{31} = 0.5$. Under this policy, we randomly stay or move in each state, and has a 50% probability of receiving a reward. The adversary ν has no power because π is the same for all states. In this situation, $V(S_1) = V(S_2) = V(S_3) = \frac{0.5}{1-0.99} = 50$ for both MDP and SA-MDP.
- **Deterministic Policies for SA-MDP.** Now we consider all $2^3 = 8$ possible deterministic policies for SA-MDP. Note that if for any state S_i we have $p_{i1} = 0$ and another state S_j we have $p_{j1} = 1$, we always have $V(S_1) = V(S_2) = V(S_3) = 0$. This is because we can set $\nu(S_1) = S_j$, $\nu(S_2) = S_i$ and $\nu(S_3) = S_i$ and always receive a 0 reward. Thus the only two possible other policies are $p_{11} = p_{21} = p_{31} = 0$ and $p_{11} = p_{21} = p_{31} = 1$, respectively. For $p_{11} = p_{21} = p_{31} = 1$ we have $V(S_1) = 0$, $V(S_2) = V(S_3) = 100$ as we always take A_1 and never transit to other states; for $p_{11} = p_{21} = p_{31} = 0$, we circulate through all three states and only receive a reward when we leave A_1 . We have $V(S_1) = \frac{1}{1-\gamma^3} \approx 33.67$, $V(S_2) = \frac{\gamma^2}{1-\gamma^3} \approx 33.00$ and $V(S_3) = \frac{\gamma}{1-\gamma^3} \approx 33.33$.

Figure 7, 8, 9 give the graph of $V(S_1)$, $V(S_2)$ and $V(S_3)$ under three different settings of p_{11} . The figures are generated using Algorithm 1.

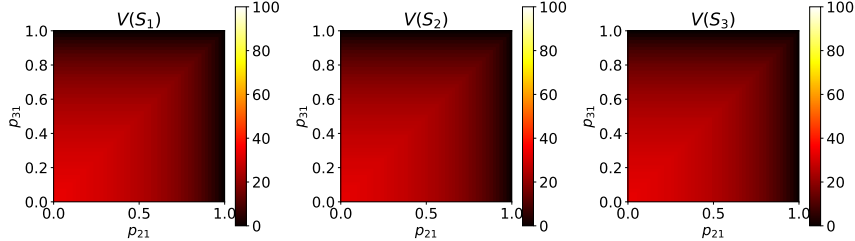


Figure 7: Value functions when $p_{11} = 0$, with $p_{21} \in [0, 1]$, $p_{31} \in [0, 1]$

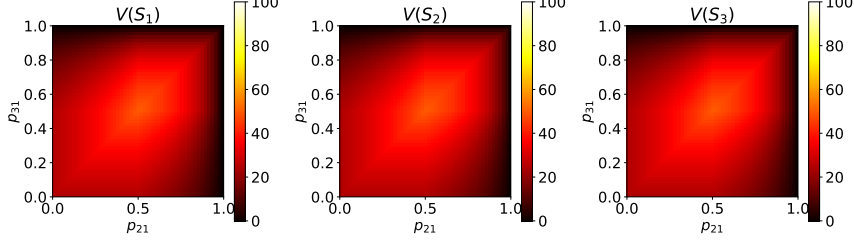


Figure 8: Value functions when $p_{11} = 0.5$, with different $p_{21} \in [0, 1]$, $p_{31} \in [0, 1]$

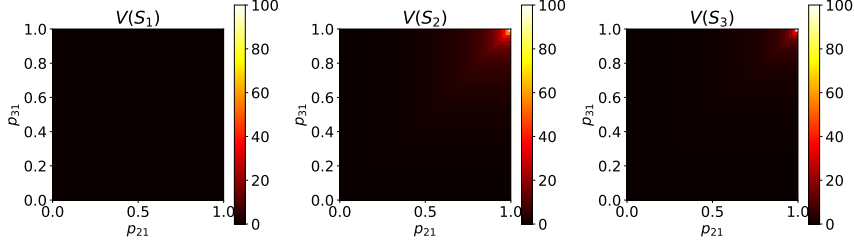


Figure 9: Value functions when $p_{11} = 1.0$, with different $p_{21} \in [0, 1]$, $p_{31} \in [0, 1]$

B Proofs for State-Adversarial Markov Decision Process

Theorem 1 (Bellman equations for fixed π and ν). *Given $\pi : \mathcal{S} \rightarrow \mathcal{P}(\mathcal{A})$ and $\nu : \mathcal{S} \rightarrow \mathcal{S}$, we have*

$$\begin{aligned}\tilde{V}_\nu^\pi(s) &= \sum_{a \in \mathcal{A}} \pi(a|\nu(s)) \sum_{s' \in \mathcal{S}} p(s'|s, a) \left[R(s, a, s') + \gamma \tilde{V}_\nu^\pi(s') \right] \\ \tilde{Q}_\nu^\pi(s, a) &= \sum_{s' \in \mathcal{S}} p(s'|s, a) \left[R(s, a, s') + \gamma \sum_{a' \in \mathcal{A}} \pi(a'|\nu(s')) \tilde{Q}_\nu^\pi(s', a') \right].\end{aligned}$$

Proof. Based on the definition of $\tilde{V}_\nu^\pi(s)$:

$$\begin{aligned}\tilde{V}_\nu^\pi(s) &= \mathbb{E}_{\pi \circ \nu} \left[\sum_{k=0}^{\infty} \gamma^k r_{t+k+1} | s_t = s \right] \\ &= \mathbb{E}_{\pi \circ \nu} \left[r_{t+1} + \gamma \sum_{k=0}^{\infty} \gamma^k r_{t+k+2} | s_t = s \right] \\ &= \sum_{a \in \mathcal{A}} \pi(a|\nu(s)) \sum_{s' \in \mathcal{S}} p(s'|s, a) \left[r_{t+1} + \gamma \mathbb{E}_{\pi \circ \nu} \left[\sum_{k=0}^{\infty} \gamma^k r_{t+k+2} | s_{t+1} = s' \right] \right] \\ &= \sum_{a \in \mathcal{A}} \pi(a|\nu(s)) \sum_{s' \in \mathcal{S}} p(s'|s, a) \left[R(s, a, s') + \gamma \tilde{V}_\nu^\pi(s') \right]\end{aligned}\tag{9}$$

The recursion for $\tilde{Q}_\nu^\pi(s, a)$ can be derived similarly. Additionally, we note the following useful relationship between $\tilde{V}_\nu^\pi(s)$ and $\tilde{Q}_\nu^\pi(s, a)$:

$$\tilde{V}_\nu^\pi(s) = \sum_{a \in \mathcal{A}} \pi(a|\nu(s)) \tilde{Q}_\nu^\pi(s, a)\tag{10}$$

□

First we show that finding the optimal adversary ν^* given a fixed π for a SA-MDP can be cast into the problem of finding an optimal policy in a regular MDP.

Lemma 1 (Equivalence of finding optimal adversary in SA-MDP and finding optimal policy in MDP). *Given a SA-MDP $M = (\mathcal{S}, \mathcal{A}, R, p)$ and a fixed policy π , there exists a MDP $\hat{M} = (\mathcal{S}, \hat{\mathcal{A}}, \hat{R}, \hat{p})$ such that the optimal policy of \hat{M} is the optimal adversary ν for SA-MDP given the fixed π .*

Proof. For a SA-MDP $M = (\mathcal{S}, \mathcal{A}, R, p)$ and a fixed policy π , we define a regular MDP $\hat{M} = (\mathcal{S}, \hat{\mathcal{A}}, \hat{R}, \hat{p})$ such that $\hat{\mathcal{A}} = \mathcal{S}$, and ν is the policy for \hat{M} . At each state s , our policy ν gives a probability distribution $\nu(\cdot|s) \in \mathcal{P}(\hat{\mathcal{A}}) = \mathcal{P}(\mathcal{S})$ indicating that we perturb a state s to \hat{s} with probability $\nu(\hat{s}|s)$ in the SA-MDP M .

For \hat{M} , the reward function is defined as:

$$\hat{R}(s, \hat{a}, s') = \begin{cases} -\frac{\sum_{a \in \mathcal{A}} \pi(a|\hat{a}) p(s'|s, a) R(s, a, s')}{\sum_{a \in \mathcal{A}} \pi(a|\hat{a}) p(s'|a, s)} & \text{for } s, s' \in \mathcal{S} \text{ and } \hat{a} \in B(s) \subset \hat{\mathcal{A}} = \mathcal{S}, \\ -\infty & \text{for } s, s' \in \mathcal{S} \text{ and } \hat{a} \notin B(s). \end{cases} \quad (11)$$

The above definition is based on the following conditional probability which marginalizes π :

$$\begin{aligned} p(r|s, \hat{a}, s') &= \frac{p(r, s' | s, \hat{a})}{p(s' | s, \hat{a})} \\ &= \frac{\sum_a p(r, s' | a, s, \hat{a}) \pi(a | s, \hat{a})}{\sum_a p(s' | a, s, \hat{a}) \pi(a | s, \hat{a})} \\ &= \frac{\sum_a p(r, s' | a, s) \pi(a | \hat{a})}{\sum_a p(s' | a, s) \pi(a | \hat{a})} \\ &= \frac{\sum_a p(r | s', a, s) p(s' | a, s) \pi(a | \hat{a})}{\sum_a p(s' | a, s) \pi(a | \hat{a})} \end{aligned}$$

Considering that $p(r = R(S, A, S') | s' = S', a = A, s = S) = 1.0$ and 0 otherwise, and taking an expectation over r yields the first case in (11). For $\hat{a} \notin B(s)$, we simply use a negative infinity reward to prevent the adversary taking that action.

The transition probability \hat{p} is defined as

$$\hat{p}(s'|s, \hat{a}) = \sum_{a \in \mathcal{A}} \pi(a|\hat{a}) p(s'|s, a) \quad \text{for } s, s' \in \mathcal{S} \text{ and } \hat{a} \in \hat{\mathcal{A}} = \mathcal{S}.$$

Then we can get the value function \hat{V}_ν^π of this MDP for any policy ν not obtaining $-\infty$ reward (never taking an action $\hat{a} \notin B(s)$):

$$\begin{aligned} \hat{V}_\nu^\pi(s) &:= \mathbb{E}_{\hat{p}, \nu} \left[\sum_{k=0}^{\infty} \gamma^k \hat{r}_{t+k+1} | s_t = s \right] \\ &= \mathbb{E}_{\hat{p}, \nu} \left[\hat{r}_{t+1} + \gamma \sum_{k=0}^{\infty} \gamma^k \hat{r}_{t+k+2} | s_t = s \right] \\ &= \sum_{\hat{a} \in \mathcal{S}} \nu(\hat{a}|s) \sum_{s' \in \mathcal{S}} \hat{p}(s'|s, \hat{a}) \left[\hat{R}(s, \hat{a}, s') + \gamma \mathbb{E}_{\hat{p}, \nu} \left[\sum_{k=0}^{\infty} \gamma^k \hat{r}_{t+k+2} | s_{t+1} = s' \right] \right] \\ &= \sum_{\hat{a} \in \mathcal{S}} \nu(\hat{a}|s) \sum_{s' \in \mathcal{S}} \hat{p}(s'|s, \hat{a}) \left[\hat{R}(s, \hat{a}, s') + \gamma \hat{V}_\nu^\pi(s') \right] \end{aligned} \quad (12)$$

According to MDP theory [46], we know that the \hat{M} has an optimal policy ν^* , which satisfies $\hat{V}_{\nu^*}^\pi(s) \geq \hat{V}_\nu^\pi(s)$ for $\forall s, \forall \nu$. We also know that this ν^* is deterministic and assigns a unit mass probability for the optimal action in $B(s)$, because if a is not in $B(s)$ the reward is $-\infty$, and this policy cannot be an optimal policy.

So from now on in this proof we only study policies in $N := \{\nu : \forall s, \exists \hat{a} \in B(s), \nu(\hat{a}|s) = 1\}$. Note that all policies in N are deterministic and this class of policies consists ν^* . Also, N is consistent

with the class of policies studied in Theorem 1. We denote the deterministic action \hat{a} chosen by a $\nu \in N$ at s as $\nu(s)$. Then for $\forall \nu \in N$, we have

$$\begin{aligned}\hat{V}_\nu^\pi(s) &= \sum_{s' \in \mathcal{S}} \hat{p}(s'|s, \nu(s)) \left[\hat{R}(s, \hat{a}, s') + \gamma \hat{V}_\nu^\pi(s') \right] \\ &= \sum_{s' \in \mathcal{S}} \sum_{a \in \mathcal{A}} \pi(a|\hat{a}) p(s'|s, a) \left[-\frac{\sum_{a \in \mathcal{A}} \pi(a|\hat{a}) p(s'|s, a) R(s, a, s')}{\sum_{a \in \mathcal{A}} \pi(a|\hat{a}) p(s'|s, a)} + \gamma \hat{V}_\nu^\pi(s') \right] \\ &= \sum_{a \in \mathcal{A}} \pi(a|\nu(s)) \sum_{s' \in \mathcal{S}} p(s'|s, a) \left[-R(s, a, s') + \gamma \hat{V}_\nu^\pi(s') \right],\end{aligned}\tag{13}$$

or

$$-\hat{V}_\nu^\pi(s) = \sum_{a \in \mathcal{A}} \pi(a|\nu(s)) \sum_{s' \in \mathcal{S}} p(s'|s, a) \left[R(s, a, s') + \gamma (-\hat{V}_\nu^\pi(s')) \right].\tag{14}$$

Comparing (14) and (9), we know that $-\hat{V}_\nu^\pi = \tilde{V}_\nu^\pi$ for any $\nu \in N$. Then the optimal value function $\hat{V}_{\nu^*}^\pi$ satisfies:

$$\begin{aligned}\hat{V}_{\nu^*}^\pi(s) &= \max_{\hat{a} \in B(s)} \sum_{s' \in \mathcal{S}} \hat{p}(s'|s, \hat{a}) \left[\hat{R}(s, \hat{a}, s') + \gamma \hat{V}_{\nu^*}^\pi(s') \right] \\ &= \max_{s_\nu \in B(s)} \sum_{a \in \mathcal{A}} \pi(a|s_\nu) \sum_{s' \in \mathcal{S}} p(s'|s, a) \left[-R(s, a, s') + \gamma \hat{V}_{\nu^*}^\pi(s') \right],\end{aligned}\tag{15}$$

where we denote the action \hat{a} taken at s as s_ν . So for ν^* , since $-\hat{V}_{\nu^*}^\pi = \tilde{V}_{\nu^*}^\pi$, we have

$$\tilde{V}_{\nu^*}^\pi(s) = \min_{\hat{a} \in B(s)} \sum_{a \in \mathcal{A}} \pi(a|\hat{a}) \sum_{s' \in \mathcal{S}} p(s'|s, a) \left[R(s, a, s') + \gamma \tilde{V}_{\nu^*}^\pi(s') \right],\tag{16}$$

and $\tilde{V}_{\nu^*}^\pi(s) \leq \tilde{V}_\nu^\pi(s)$ for $\forall s, \forall \nu \in N$. Hence ν^* is also the optimal ν for \tilde{V}_ν^π . \square

Lemma 1 gives many good properties for the optimal adversary. First, an optimal adversary always exists. Second, we do not need to consider stochastic adversaries as there always exists an optimal deterministic adversary. Additionally, showing Bellman contraction for finding the optimal adversary can be done similarly as in obtaining the optimal policy in a regular MDP, as shown in the proof of Theorem 2.

Theorem 2 (Bellman contraction for optimal adversary). *Define Bellman operator $\mathcal{L} : \mathbb{R}^{|\mathcal{S}|} \rightarrow \mathbb{R}^{|\mathcal{S}|}$,*

$$(\mathcal{L}\tilde{V}^\pi)(s) = \min_{s_\nu \in B(s)} \sum_{a \in \mathcal{A}} \pi(a|s_\nu) \sum_{s' \in \mathcal{S}} p(s'|s, a) \left[R(s, a, s') + \gamma \tilde{V}^\pi(s') \right].\tag{17}$$

The Bellman equation for optimal adversary ν^ can be written as: $\tilde{V}_{\nu^*}^\pi = \mathcal{L}\tilde{V}_{\nu^*}^\pi$. Additionally, \mathcal{L} is a contraction that converges to $\tilde{V}_{\nu^*}^\pi$.*

Proof. Based on Lemma 1, this proof is technically similar to the proof of “optimal Bellman equation”

in regular MDPs, where max over π is replaced by min over ν . By the definition of $\tilde{V}_{\nu^*}^\pi(s)$,

$$\begin{aligned}
\tilde{V}_{\nu^*}^\pi(s) &= \min_\nu \tilde{V}_\nu^\pi(s) \\
&= \min_\nu \mathbb{E}_{\pi \circ \nu} \left[\sum_{k=0}^{\infty} \gamma^k r_{t+k+1} | s_t = s \right] \\
&= \min_\nu \mathbb{E}_{\pi \circ \nu} \left[r_{t+1} + \gamma \sum_{k=0}^{\infty} \gamma^k r_{t+k+2} | s_t = s \right] \\
&= \min_\nu \sum_{a \in \mathcal{A}} \pi(a | \nu(s)) \sum_{s' \in \mathcal{S}} p(s' | s, a) \left[r_{t+1} + \gamma \mathbb{E}_{\pi \circ \nu} \left[\sum_{k=0}^{\infty} \gamma^k r_{t+k+2} | s_{t+1} = s' \right] \right] \\
&= \min_{s_\nu \in B_\nu(s)} \sum_{a \in \mathcal{A}} \pi(a | s_\nu) \sum_{s' \in \mathcal{S}} p(s' | s, a) \left[r_{t+1} + \gamma \min_\nu \mathbb{E}_{\pi \circ \nu} \left[\sum_{k=0}^{\infty} \gamma^k r_{t+k+2} | s_{t+1} = s' \right] \right] \\
&= \min_{s_\nu \in B_\nu(s)} \sum_{a \in \mathcal{A}} \pi(a | s_\nu) \sum_{s' \in \mathcal{S}} p(s' | s, a) \left[r_{t+1} + \gamma \tilde{V}_{\nu^*}^\pi(s') \right]
\end{aligned}$$

This is the Bellman equation for the optimal adversary ν^* ; ν^* is a fixed point of the Bellman operator \mathcal{L} .

Now we show the Bellman operator is a contraction. We have, if $\mathcal{L}\tilde{V}_{\nu_1}^\pi(s) \geq \mathcal{L}\tilde{V}_{\nu_2}^\pi(s)$,

$$\begin{aligned}
&\mathcal{L}\tilde{V}_{\nu_1}^\pi(s) - \mathcal{L}\tilde{V}_{\nu_2}^\pi(s) \\
&\leq \max_{s_\nu \in B_\nu(s)} \left\{ \sum_{a \in \mathcal{A}} \pi(a | s_\nu) \sum_{s' \in \mathcal{S}} p(s' | s, a) \left[R(s, a, s') + \gamma \tilde{V}_{\nu_1}^\pi(s') \right] \right. \\
&\quad \left. - \sum_{a \in \mathcal{A}} \pi(a | s_\nu) \sum_{s' \in \mathcal{S}} p(s' | s, a) \left[R(s, a, s') + \gamma \tilde{V}_{\nu_2}^\pi(s') \right] \right\} \\
&= \gamma \max_{s_\nu \in B_\nu(s)} \sum_{a \in \mathcal{A}} \pi(a | s_\nu) \sum_{s' \in \mathcal{S}} p(s' | s, a) [\tilde{V}_{\nu_1}^\pi(s') - \tilde{V}_{\nu_2}^\pi(s')] \\
&\leq \gamma \max_{s_\nu \in B_\nu(s)} \sum_{a \in \mathcal{A}} \pi(a | s_\nu) \sum_{s' \in \mathcal{S}} p(s' | s, a) \|\tilde{V}_{\nu_1}^\pi - \tilde{V}_{\nu_2}^\pi\|_\infty \\
&= \gamma \|\tilde{V}_{\nu_1}^\pi - \tilde{V}_{\nu_2}^\pi\|_\infty
\end{aligned}$$

The first inequality comes from the fact that

$$\min_{x_1} f(x_1) - \min_{x_2} g(x_2) \leq f(x_2^*) - g(x_2^*) \leq \max_x (f(x) - g(x)),$$

where $x_2^* = \arg \min_{x_2} g(x_2)$. Similarly, we can prove $\mathcal{L}\tilde{V}_{\nu_2}^\pi(s) - \mathcal{L}\tilde{V}_{\nu_1}^\pi(s) \leq \|\tilde{V}_{\nu_1}^\pi - \tilde{V}_{\nu_2}^\pi\|_\infty$ if $\mathcal{L}\tilde{V}_{\nu_2}^\pi(s) > \mathcal{L}\tilde{V}_{\nu_1}^\pi(s)$. Hence

$$\|\mathcal{L}\tilde{V}_{\nu_1}^\pi(s) - \mathcal{L}\tilde{V}_{\nu_2}^\pi(s)\|_\infty = \max_s |\mathcal{L}\tilde{V}_{\nu_1}^\pi(s) - \mathcal{L}\tilde{V}_{\nu_2}^\pi(s)| \leq \gamma \|\tilde{V}_{\nu_1}^\pi - \tilde{V}_{\nu_2}^\pi\|_\infty.$$

Then according to the Banach fixed-point theorem, since $0 < \gamma < 1$, \tilde{V}_ν^π converges to a unique fixed point, and this fixed point is $\tilde{V}_{\nu^*}^\pi$. □

A direct consequence of Theorem 2 is the policy evaluation algorithm (Algorithm 1) for SA-MDP, which obtains the values for each state under optimal adversary for a fixed policy π . For both Lemma 1 and Theorem 2, we only consider a fixed policy π , and in this setting finding an optimal adversary is not difficult. However, finding an optimal π under the optimal adversary is more challenging, as we can see in Section A, given the white-box attack setting where the adversary knows π and can choose optimal perturbations accordingly, an optimal policy for MDP can only receive zero rewards under optimal adversary. We now show two intriguing properties for optimal policies in SA-MDP:

Algorithm 1 Policy Evaluation for SA-MDP

Input: Policy π , convergence threshold ε
Output: Values for policy π , $V_{\nu^*}^\pi(s)$

Initialize $V(s) \leftarrow 0$ for all $s \in \mathcal{S}$

repeat

$\Delta \leftarrow 0$

for all $s \in \mathcal{S}$ **do**

$v \leftarrow \infty, v_0 \leftarrow V(s)$

for all $s_\nu \in B(s)$ **do**

$v' \leftarrow \sum_{a \in \mathcal{A}} \pi(a|s_\nu) \sum_{s' \in \mathcal{S}} p(s'|s, a) \cdot [R(s, a, s') + \gamma \tilde{V}^\pi(s')]$

$v \leftarrow \min(v, v')$

end for

$V(s) \leftarrow v$

$\Delta \leftarrow \max(\Delta, |v_0 - V(s)|)$

end for

until $\Delta < \varepsilon$

$V_{\nu^*}^\pi(s) \leftarrow V(s)$

Theorem 3. *There exists an SA-MDP and some stochastic policy $\pi \in \Pi_{MR}$ such that we cannot find a better deterministic policy $\pi' \in \Pi_{MD}$ satisfying $\tilde{V}_{\nu^*(\pi')}^\pi(s) \geq \tilde{V}_{\nu^*(\pi)}^\pi(s)$ for all $s \in \mathcal{S}$.*

Proof. Proof by giving a counter example that no deterministic policy can be better than a random policy. The SA-MDP example in section A provided such a counter example: all 8 possible deterministic policies are no better than the stochastic policy $p_{11} = p_{21} = p_{31} = 0.5$. \square

Theorem 4. *Under the optimal ν^* , an optimal policy $\pi^* \in \Pi_{MR}$ does not always exist for SA-MDP.*

Proof. The SA-MDP example in section A does not have an optimal policy. For π_1 where $p_{11} = p_{21} = p_{31} = 1$ we have $V^{\pi_1}(S_1) = 0, V^{\pi_1}(S_2) = V^{\pi_1}(S_3) = 100$. This policy is not an optimal policy since we have π_2 where $p_{11} = p_{21} = p_{31} = 0.5$ that can achieve $V^{\pi_2}(S_1) = V^{\pi_2}(S_2) = V^{\pi_2}(S_3) = 50$ and $V^{\pi_2}(S_1) > V^{\pi_1}(S_1)$.

An optimal policy π , if exists, must be better than π_1 and have $V^\pi(S_1) > 0, V^\pi(S_2) = V^\pi(S_3) = 100$. In order to achieve $V^\pi(S_2) = V^\pi(S_3) = 100$, we must set $p_{21} = p_{31} = 1$ since it is the only possible way to start from S_2 and S_3 and receive +1 reward for every step. We can still change p_{11} to probabilities other than 1, however if $p_{11} < 1$ the adversary can set $\nu(S_2) = \nu(S_3) = S_1$ and reduce $V^\pi(S_2)$ and $V^\pi(S_3)$. Thus, no policy better than π_1 exists, and since π_1 is not an optimal policy, no optimal policy exists. \square

Theorem 3 and Theorem 4 show that the classic definition of optimality is probably not suitable for SA-MDP. Further works can study how to obtain optimal policies for SA-MDP under some alternative definition of optimality.

Theorem 5. *Given a policy π for a non-adversarial MDP. Under the optimal adversary ν in SA-MDP, for all $s \in \mathcal{S}$ we have*

$$\max_{s \in \mathcal{S}} \{V^\pi(s) - \tilde{V}_{\nu^*}^\pi(s)\} \leq \alpha \max_{s \in \mathcal{S}} \max_{\hat{s} \in B(s)} D_{TV}(\pi(\cdot|s), \pi(\cdot|\hat{s})) \quad (18)$$

where $D_{TV}(\pi(\cdot|s), \pi(\cdot|\hat{s}))$ is the total variation distance between $\pi(\cdot|s)$ and $\pi(\cdot|\hat{s})$, and $\alpha := 2[1 + \frac{\gamma}{(1-\gamma)^2}] \max_{(s,a,s') \in \mathcal{S} \times \mathcal{A} \times \mathcal{S}} |R(s, a, s')|$ is a constant that does not depend on π .

Proof. Our proof is based on Theorem 1 in Achiam et al. [1]. In fact, many works in the literature have proved similar results under different scenarios [24, 45]. For an arbitrary starting state s_0 and two

arbitrary policies π and π' , Theorem 1 in Achiam et al. [1] gives an upper bound of $V^\pi(s_0) - V^{\pi'}(s_0)$. The bound is given by

$$\begin{aligned} V^\pi(s_0) - V^{\pi'}(s_0) &\leq -\mathbb{E}_{\substack{s \sim d_{s_0}^\pi \\ a \sim \pi(\cdot|s) \\ s' \sim p(\cdot|a,s)}} \left[\left(\frac{\pi'(a|s)}{\pi(a|s)} - 1 \right) R(s, a, s') \right] \\ &\quad + \frac{2\gamma}{(1-\gamma)^2} \max_s \left\{ \mathbb{E}_{\substack{a \sim \pi'(\cdot|s) \\ s' \sim p(\cdot|a,s)}} [R(s, a, s')] \right\} \mathbb{E}_{s \sim d_{s_0}^\pi} [\text{D}_{TV}(\pi(\cdot|s), \pi'(\cdot|s))], \end{aligned} \quad (19)$$

where $d_{s_0}^\pi$ is the discounted future state distribution from s_0 , defined as

$$d_{s_0}^\pi(s) := (1-\gamma) \sum_{t=0}^{\infty} \gamma^t \Pr(s_t = s | \pi, s_0). \quad (20)$$

Note that in Theorem 1 of Achiam et al. [1], the author proved a general form with an arbitrary function f and we assume $f \equiv 0$ in our proof. We also assume the starting state is deterministic, so J^π in Achiam et al. [1] is replaced by $V^\pi(s_0)$. Then we simply need to bound both terms on the right hand side of (19).

For the first term we know that

$$\begin{aligned} -\mathbb{E}_{\substack{s \sim d_{s_0}^\pi \\ a \sim \pi(\cdot|s) \\ s' \sim p(\cdot|a,s)}} \left[\left(\frac{\pi'(a|s)}{\pi(a|s)} - 1 \right) R(s, a, s') \right] &= \sum_s d_{s_0}^\pi(s) \sum_a [\pi(a|s) - \pi'(a|s)] \sum_{s'} p(s'|s, a) R(s, a, s') \\ &\leq \sum_s d_{s_0}^\pi(s) \sum_a |\pi(a|s) - \pi'(a|s)| \left| \sum_{s'} p(s'|s, a) R(s, a, s') \right| \\ &\leq \max_{s, a, s'} |R(s, a, s')| \max_s \left\{ \sum_a |\pi(a|s) - \pi'(a|s)| \right\} \\ &= 2 \max_{s, a, s'} |R(s, a, s')| \max_s \text{D}_{TV}(\pi(\cdot|s), \pi'(\cdot|s)) \end{aligned} \quad (21)$$

The second term is bounded by

$$\begin{aligned} \frac{2\gamma}{(1-\gamma)^2} \max_s \left\{ \mathbb{E}_{\substack{a \sim \pi'(\cdot|s) \\ s' \sim p(\cdot|a,s)}} [R(s, a, s')] \right\} \mathbb{E}_{s \sim d_{s_0}^\pi} [\text{D}_{TV}(\pi(\cdot|s), \pi'(\cdot|s))] \\ \leq \frac{2\gamma}{(1-\gamma)^2} \max_{s, a, s'} |R(s, a, s')| \max_s \text{D}_{TV}(\pi(\cdot|s), \pi'(\cdot|s)) \end{aligned} \quad (22)$$

Therefore, the RHS of (19) is bounded by $\alpha \max_s \text{D}_{TV}(\pi(\cdot|s), \pi'(\cdot|s))$, where

$$\alpha = 2 \left[1 + \frac{\gamma}{(1-\gamma)^2} \right] \max_{s, a, s'} |R(s, a, s')| \quad (23)$$

Finally, we simply let $\pi'(\cdot|s) := \pi(\cdot|\nu^*(s))$ and the proof is complete. \square

Before proving 6 we first give a technical lemma about the total variation distance between two multi-variate Gaussian distributions with the same variance.

Lemma 2. *Given two multi-variate Gaussian distributions $X_1 \sim \mathcal{N}(\mu_1, \sigma^2 I_n)$ and $X_2 \sim \mathcal{N}(\mu_2, \sigma^2 I_n)$, $\mu_1, \mu_2 \in \mathbb{R}^n$, define $d = \|\mu_2 - \mu_1\|_2$. We have $\text{D}_{TV}(X_1, X_2) = \sqrt{\frac{2}{\pi} \frac{d}{\sigma}} + O(d^3)$.*

Proof. Denote probability density of X_1 and X_2 as f_1 and f_2 , and denote $a = \frac{\mu_2 - \mu_1}{d}$ as the normal vector of the perpendicular bisector line between μ_1 and μ_2 . Due to the symmetry of Gaussian distribution, $f_1(x) - f_2(x)$ is positive for all x where $a^\top x - a^\top \mu_1 - \frac{d}{2} > 0$ and negative for all x on the other symmetric side. When $a^\top x - a^\top \mu_1 - \frac{d}{2} > 0$, $\int_{x \in \mathbb{R}^n} [f_1(x) - f_2(x)] dx = \Phi\left(\frac{d}{2\sigma}\right) - (1 - \Phi\left(\frac{d}{2\sigma}\right)) = 2\Phi\left(\frac{d}{2\sigma}\right) - 1$. Thus,

$$\begin{aligned} D_{TV}(X_1, X_2) &= \int_{x \in \mathbb{R}^n} |f_1(x) - f_2(x)| dx \\ &= 2 \int_{a^\top x - a^\top \mu_1 - \frac{d}{2} > 0} (f_1(x) - f_2(x)) dx \\ &= 2(\Phi\left(\frac{d}{2\sigma}\right) - (1 - \Phi\left(\frac{d}{2\sigma}\right))) \\ &= 2(2\Phi\left(\frac{d}{2\sigma}\right) - 1) \end{aligned}$$

Then we use the Taylor series for $\Phi(x)$ at $x = 0$:

$$\Phi(x) = \frac{1}{2} + \frac{1}{\sqrt{2\pi}} \sum_{n=0}^{\infty} \frac{(-1)^n x^{2n+1}}{2^n n! (2n+1)}$$

Since we consider the case where d is small, we only keep the first order term and obtain:

$$D_{TV}(X_1, X_2) = \sqrt{\frac{2}{\pi}} \frac{d}{\sigma} + O(d^3)$$

□

Theorem 6. $D_{TV}(\bar{\pi}(\cdot|s), \bar{\pi}(\cdot|\hat{s})) = \sqrt{2/\pi} \frac{d}{\sigma} + O(d^3)$, where $d = \|\pi(s) - \pi(\hat{s})\|_2$.

Proof. This theorem is a special case of Lemma 2 where $X_1 = \bar{\pi}(\cdot|s)$, $X_2 = \bar{\pi}(\cdot|s')$ and $X_1 \sim \mathcal{N}(\pi(s), \sigma^2 I)$, $X_2 \sim \mathcal{N}(\pi(s'), \sigma^2 I)$. □

C Additional details for adversarial attacks on state observations

C.1 More details on the Critic based attack

In Section 3.5 we discuss critic based attack [43] as a baseline. This attack requires a Q function $Q(s, a)$ to find the best perturbed state. In Algorithm 2 we present our “corrected” critic based attack based on [43]:

Note that in Algorithm 4 of [43], they use the gradient $\nabla Q_s(s, \pi(s)) = \frac{\partial Q}{\partial s} + \frac{\partial Q}{\partial \pi} \frac{\partial \pi}{\partial s}$ which essentially attempts to minimize $Q(\hat{s}, \pi(\hat{s}))$, but they then sample randomly along this gradient direction to find the best \hat{s} that minimizes $Q(s_0, \pi(\hat{s}))$. Our corrected formulation directly minimizes $Q(s_0, \pi(\hat{s}))$ using this gradient instead $\nabla Q_s(s_0, \pi(s)) = \frac{\partial Q}{\partial \pi} \frac{\partial \pi}{\partial s}$.

For PPO, since there is no $Q(s, a)$ available during training, we extend [43] to perform attack relying on $V(s)$: we find a state \hat{s} that minimizes $V(\hat{s})$. Unfortunately, it does not match our setting of perturbing state observations; it looks for a state \hat{s} that has the worst value (i.e., taking action $\pi(\hat{s})$ in state \hat{s} is bad), but taking the action $\pi(\hat{s})$ at state s_0 does not necessarily trigger a low reward action, because $V(\hat{s}) = \max_a Q(\hat{s}, a) \neq \max_a Q(s_0, a)$. Thus, in Table 1 we can observe that critic based attack typically does not work very well for PPO agents.

Algorithm 2 Critic based attack [43]

Input: A policy function π under attack, a corresponding $Q(s, a)$ network, and a initial state s_0 , T is the number of attack steps, η is the step size, \underline{s} and \bar{s} are valid lower and upper range of s .

for $t = 1$ to T **do**

$g_t = \nabla Q_{s_{t-1}}(s_0, \pi(s_{t-1})) = \frac{\partial Q}{\partial \pi} \frac{\partial \pi}{\partial s_{t-1}}$

$g_t \leftarrow \text{proj}(g_t)$ ▷ project g_t according to norm constraint of s ; for ℓ_∞ norm simply take the sign

$s_t \leftarrow s_{t-1} - \eta g_t$

$s_t \leftarrow \min(\max(s_t, \underline{s}), \bar{s})$

end for

Output: An adversarial state $\hat{s} := s_T$

C.2 More details on the Maximal Action Difference (MAD) attack

We present the full algorithm of MAD in Algorithm 3. It is a relatively simple attack by directly maximizing a KL-divergence using SGLD, yet it usually outperforms random attack and critic attack on some environments (e.g., see Figure 11).

Algorithm 3 Maximal Action Difference (MAD) Attack (a critic-independent attack)

Input: A policy function π under attack, and a initial state s_0 , T is the number of attack steps, η is the step size, β is the (inverse) temperature parameter for SGLD, \underline{s} and \bar{s} are valid lower and upper range of s .

Define loss function $L_{\text{MAD}}(s) = -D_{\text{KL}}(\pi(\cdot|s_0) \parallel \pi(\cdot|s))$

for $t = 1$ to T **do**

Sample $\xi \sim \mathcal{N}(0, 1)$

$g_t = \nabla L_{\text{MAD}}(s_{t-1}) + \sqrt{\frac{2}{\beta \eta}} \xi$

$g_t \leftarrow \text{proj}(g_t)$ ▷ project g_t according to norm constraint of s ; for ℓ_∞ norm simply take the sign

$s_t \leftarrow s_{t-1} - \eta g_t$

$s_t \leftarrow \min(\max(s_t, \underline{s}), \bar{s})$

end for

Output: An adversarial state $\hat{s} := s_T$

C.3 More details on the Robust Sarsa attack

Algorithm 4 gives the full procedure of the Robust Sarsa attack. We collect trajectories of the agents and then optimize the ordinary temporal difference (TD) loss along with a robust objective $L_{\text{robust}}(\theta)$. $L_{\text{robust}}(\theta)$ constrains that when an input action a is slightly changed, the value $Q_{\text{RS}}^\pi(s, a)$ should not change significantly. We set the perturbation set $B_p(a, \epsilon)$ to be a ℓ_p norm ball with radius ϵ around an action a . We gradually increase ϵ from 0 to ϵ_{max} during training to learn a critic that is increasingly robust. The inner maximization of $L_{\text{robust}}(\theta)$ is upper bounded by convex relaxations of neural networks, which we will introduce in section D. Once the inner maximization is eliminated, we solve the final objective use regular first order optimization methods. In our attacks to DDPG and PPO, we try multiple regularization parameter λ_{RS} to find the best Sarsa model that achieves *lowest* attack rewards.

Although it is beyond the scope of this paper, RS attack can also be used as a blackbox attack when perturbing the actions, as $Q_{\theta_{\text{RS}}}^\pi$ can be learned by observing the environment and the agent without any internal information of the agent. Then, using the robust critic we learned, black-box attacks can be performed on action space by solving $\min Q_{\theta_{\text{RS}}}^\pi(s, a)$ with a norm constrained a .

We provide some empirical justifications for the necessity of using a robust objective. For both PPO and DDPG, we conduct attacks using a Sarsa network trained with and without the robustness

Algorithm 4 Train a Robust Sarsa network for critic-independent attack

Input: Any policy function π under attack, T is the number of training steps, and an epsilon schedule

ϵ_t

Initialize $Q_{RS}^\pi(s, a)$ to be a random network

for $t = 1$ to T **do**

Run the agent with policy π and collect a batch of N steps: $\{s_i, a_i, r_i, s'_i, a'_i\}, i \in [N]$

$$L_{TD}(\theta) = \sum_{i \in [N]} [r_i + \gamma Q_{RS}^\pi(s'_i, a'_i) - Q_{RS}^\pi(s_i, a_i)]^2$$

$$L_{robust}(\theta) = \sum_{i \in [N]} \max_{\hat{a} \in B_p(a_i, \epsilon_t)} (Q_{RS}^\pi(s_i, \hat{a}) - Q_{RS}^\pi(s_i, a_i))^2$$

$\bar{L}_{robust} = \text{ConvexRelaxUB}(L_{robust}, \theta, B_p(a_i, \epsilon_t))$, where $L_{robust}(\theta) \leq \bar{L}_{robust}(\theta)$ \triangleright Solving the inner maximization by upper bounding L_{robust} using an automatic NN convex relaxation tool

Minimize $L_{RS}(\theta) = L_{TD}(\theta) + \lambda_{RS} \bar{L}_{robust}(\theta)$ using any gradient based optimizer (e.g., Adam)

end for

Output: A robust critic function Q_{RS}^π that can be used for critic based attack.

objective, in Table 4 and Table 5, respectively. We observe that the robust objective can decrease reward further more for many settings.

Table 4: Comparison between Non-robust Sarsa attack (without the robustness objective $L_{robust}(\theta)$) and robust Sarsa attack on PPO and SA-PPO models in Table 1. The Robust Sarsa Attack Reward column is the same result presented in RS column of Table 1. We report mean reward \pm standard deviation over 50 attack episodes.

Env.	ℓ_∞ norm perturbation budget ϵ	Method	Non-robust Sarsa Attack Reward	Robust Sarsa Attack Reward
Hopper	0.05	PPO (vanilla)	3214 \pm 605	1321 \pm 189
		PPO (adv. 50%)	276 \pm 140	98 \pm 92
		PPO (adv. 100%)	14.4 \pm 4.20	11.7 \pm 4.49
		SA-PPO (SGLD)	2306 \pm 920	1675 \pm 538
		SA-PPO (Convex)	1849 \pm 786	1797 \pm 910
Walker2d	0.05	PPO (vanilla)	2847 \pm 1404	1336 \pm 654
		PPO (adv. 50%)	-10.79 \pm 0.93	-11.55 \pm 0.79
		PPO (adv. 100%)	-111.9 \pm 4.5	-114.4 \pm 4.0
		SA-PPO (SGLD)	3476 \pm 1405	2415 \pm 1451
		SA-PPO (Convex)	3481 \pm 1640	2841 \pm 1679
Humanoid	0.075	PPO (vanilla)	804 \pm 290	672 \pm 235
		PPO (adv. 50%)	166 \pm 78	98 \pm 69
		PPO (adv. 100%)	122.6 \pm 15.9	113.2 \pm 18.5
		SA-PPO (SGLD)	5025 \pm 1931	4285 \pm 2016
		SA-PPO (Convex)	4970 \pm 1786	4392 \pm 2122

Hybrid RS+MAD attack. We find that RS and MAD attack can achieve best results on different tasks in some cases. We thus combine them to form a hybrid attack, which minimizes the robust critic predicted value and in the meanwhile maximizes action differences. It can be conducted by minimizing this loss function:

$$L_{\text{Hybrid}}(\hat{s}) = \alpha_{\text{RS-MAD}} Q_{\theta_Q}(s, \pi_{\theta_{RS}}(\hat{s})) + (1 - \alpha_{\text{RS-MAD}}) L_{\text{MAD}}(\hat{s})$$

We try different values of $\alpha_{\text{RS-MAD}}$ and report the best attack (lowest reward) as the reward under this attack.

C.4 Attack for DQN

For DQN, we use the regular untargeted Projected Gradient Descent (PGD) attack in the literature [30, 43, 70]. The untargeted PGD attack with K iterations updates the state K times as follows:

$$\begin{aligned} s^{k+1} &= s^k + \eta \text{proj}[\nabla_{s^k} \mathcal{H}(Q_\theta(s^k, \cdot), a^*)], \\ s^0 &= s, \quad k = 0, \dots, K-1 \end{aligned} \tag{24}$$

Table 5: Comparison between Non-robust Sarsa attack (without the robustness objective) and robust Sarsa attack on DDPG and SA-DDPG models in Table 2. The Robust Sarsa Attack Reward column is the same result presented in the RS column of Table 2. We report mean reward \pm standard deviation over 50 attack episodes.

Env.	ℓ_∞ norm perturbation budget ϵ	Method	Non-robust Sarsa Attack Reward	Robust Sarsa Attack Reward
Ant	0.2	DDPG (vanilla)	390.18 \pm 472.07	367.74 \pm 346.33
		SA-DDPG (Convex)	2036.16 \pm 110.85	2011.44 \pm 107.82
Hopper	0.075	DDPG (vanilla)	874.35 \pm 472.85	703.97 \pm 227.82
		SA-DDPG (Convex)	3320.00 \pm 32.94	1722.20 \pm 598.55
InvertedPendulum	0.5	DDPG (vanilla)	1000.00 \pm 0.00	1000.00 \pm 0.00
		SA-DDPG (Convex)	970.36 \pm 124.24	1000.00 \pm 0.00
Reacher	1.5	DDPG (vanilla)	-19.34 \pm 3.58	-17.05 \pm 3.76
		SA-DDPG (Convex)	-11.69 \pm 4.91	-13.65 \pm 3.64
Walker2d	0.15	DDPG (vanilla)	443.44 \pm 485.36	711.50 \pm 663.04
		SA-DDPG (Convex)	3106.54 \pm 1342.82	2207.39 \pm 1266.02

where $\mathcal{H}(Q_\theta(s^k, \cdot), a^*)$ is the cross-entropy loss between the output logits of $Q_\theta(s^k, \cdot)$ and the onehot-encoded distribution of $a^* := \arg \max_a Q_\theta(s, a)$. $\text{proj}[\cdot]$ is a projection operator depending on the norm constraint of $B(s)$ and η is the learning rate. A successful untargeted PGD attack will then perturb the state to lead the Q network to output an action other than the optimal action a^* chosen at the original state s . To guarantee that the final state obtained by the attack is within an ℓ_∞ ball around s ($B_\epsilon(s) = \{\hat{s} : s - \epsilon \leq \hat{s} \leq s + \epsilon\}$), the projection $\text{proj}[\cdot]$ is a sign operator and η is typically set to $\eta = \frac{\epsilon}{K}$.

D Backgrounds for Convex Relaxation of Neural Networks

In our work, we frequently need to solve a minimax problem:

$$\min_{\theta} \max_{\phi \in \mathcal{S}} g(\theta, \phi) \quad (25)$$

One approach we discussed above is to first solve the inner maximization problem (approximately) using an optimizer like SGLD. However, due to the non-convexity of π_θ , we cannot solve the inner maximization to global maxima, and the gap between local maxima and global maxima can be large. Using convex relaxations of neural networks, we can instead find an upper bound of $\max_{\phi \in \mathcal{S}} g(\theta, \phi)$:

$$\bar{g}(\theta) \geq \max_{\phi \in \mathcal{S}} g(\theta, \phi)$$

Thus we can minimize an upper bound instead, which can guarantee the original objective (25) is minimized.

As an illustration on how to find $\bar{g}(\theta)$ using convex relaxations, following [50] we consider a simple L -layer MLP network $f(\theta, x)$ with parameters $\theta = \{(W^{(i)}, b^{(i)}), i \in \{1, \dots, L\}\}$ and activation function σ . We denote $x^{(0)} = x$ as the input, $x^{(i)}$ as the post-activation value for layer i , $z^{(i)}$ as the pre-activation value for layer i . $i \in \{1, \dots, L\}$. The output of the network $f(\theta, x)$ is $z^{(L)}$. Then, we consider the following optimization problem:

$$\max_{x \in \mathcal{S}} f(\theta, x), \quad \text{where } \mathcal{S} \text{ is the set of perturbations}$$

which is equivalent to the following optimization problem:

$$\begin{aligned} \max & \quad z^{(L)} \\ \text{s.t.} & \quad z^{(l)} = W^{(l)} x^{(l-1)} + b^{(l)}, l \in [L], \\ & \quad x^{(l)} = \sigma(z^{(l)}), l \in [L-1], \\ & \quad x^{(0)} \in \mathcal{S} \end{aligned} \quad (26)$$

In this constrained optimization problem (26), assuming \mathcal{S} is a convex set, the constraint on $z^{(l)}$ is convex (linear) and the only non-convex constraints are those for $x^{(l)}$, where a non-linear activation function is involved. Note that activation function $\sigma(z)$ itself can be a convex function, but when used as an equality constraint, the feasible solution is constrained to the *graph* of $\sigma(z)$, which is non-convex.

Previous works [68, 75, 50] propose to use convex relaxations of non-linear units to relax the non-convex constraint $x^{(l)} = \sigma(z^{(l)})$ with a convex one, $x^{(l)} = \text{convex}(\sigma(z^{(l)}))$, such that (26) can be solved efficiently. We can then obtain an *upper bound* of $f(\theta, x)$ since the constraints are relaxed.

Zhang et al. [75] gave several concrete examples (e.g., ReLU, tanh, sigmoid) on how these relaxations are formed. In the special case where linear relaxations are used, (26) can be solved efficiently and automatically (without manual derivation and implementation) for general computational graphs [72]. Generally, using the framework from Xu et al. [72] we can access an oracle function ConvexRelaxUB defined as below:

Definition 1. *Given a neural network function $f(\mathbf{X})$ where \mathbf{X} is any input for this function, and $\mathbf{X} \in \mathbb{S}$ where \mathbb{S} is the set of perturbations, the oracle function ConvexRelaxUB provided by an automatic neural network convex relaxation tool returns an upper bound \bar{f} , which satisfies:*

$$\bar{f} \geq \max_{\mathbf{X} \in \mathbb{S}} f(\mathbf{X})$$

Note that in the above definition, \mathbf{X} can be *any* input for this computation (e.g., \mathbf{X} can be s , a , or θ for a $Q_\theta(s, a)$ function). In the special case of our paper, for simplicity we define the notation ConvexRelaxUB($f, \theta, s \in B(s)$) which returns an upper bound function $\bar{f}(\theta)$ for $\max_{s \in B(s)} f(\theta, s)$.

E Robustness Certificates for Deep Reinforcement Learning

If we use the convex relaxation in Section D to train our networks, it can produce robustness certificates for our task. However in some RL tasks the certificates have interpretations different from classification tasks, as discussed in detail below.

Robustness Certificates for DQN. In DQN, the action space is finite, so we have a robustness certificate on the actions taken at each state. More specifically, at each state s , policy π 's action is certified if its corresponding Q function satisfies

$$\arg \max_a Q_\theta(s, a) = \arg \max_a Q_\theta(\hat{s}, a) = a^*, \text{ for all } \hat{s} \in B(s). \quad (27)$$

As mentioned in Section 3.4 if $u_{Q_\theta, a^*, a} \leq 0$ holds for all $\hat{s} \in B(s)$, we have

$$Q_\theta^-(\hat{s}, a, a^*) := Q_\theta(\hat{s}, a) - Q_\theta(\hat{s}, a^*) \leq 0 \quad (28)$$

is guaranteed for all $a \in \mathcal{A}$, which means that the agent's action will not change when the state observation is in $B(s)$. When the agent's action is not changed under adversarial perturbation, its reward and transition at current step will not change in the DQN setting, either.

In some settings, we find that 100% of the actions are guaranteed to be unchanged (e.g., the Pong environment in Table 3). In that case, we can in fact also certify the accumulated reward is not changed given the specific initial conditions for testing. However, it can still be challenging to certify that the agent is robust under *any* starting condition. Similarly, in classification problems many existing certified defenses [69, 38, 15, 77] can only practically guarantee robustness on a specific test set (by computing a “verified test error”), rather than on *any* input image.

Robustness Certificates for PPO and DDPG. In DDPG and PPO, the action space is continuous, hence it is not possible to certify that actions do not change under adversary. We instead seek for a

different type of guarantee, where we can upper bound the change in action given a norm bounded input perturbation:

$$U_s \geq \max_{\hat{s} \in B(s)} \|\pi_{\theta_\pi}(\hat{s}) - \pi_{\theta_\pi}(s)\| \quad (29)$$

Given a state s , we can use convex relaxations to compute an upper bound U_s . Generally speaking, if $B(s)$ is small, a robust policy desires to have a small U_s , otherwise it can be possible to find an adversarial state perturbation that greatly changes $\pi_{\theta_\pi}(\hat{s})$ and causes the agent to misbehave. However, giving certificates on accumulative rewards is still challenging, as it requires to bound reward $r(s, a)$ given a fixed state s , and a perturbed and bounded action a (bounded via (29)). Since the environment dynamics can be quite complex in practice (except for the simplest environment like InvertedPendulum), it is hard to bound reward changes given a bounded action. We leave this part as a future direction for exploration and we believe the robustness certificates (29) can be useful for future works.

F Additional details for SA-PPO

Algorithm We present the full SA-PPO algorithm in Algorithm 5. Comparing to vanilla PPO, we add a robust action regularizer which constrains the KL divergence on state perturbations. The regularizer $L_{SA}(\theta_\pi)$ can be solved using SGLD or convex relaxations of neural networks. We define the perturbation set $B(s)$ to be a ℓ_p norm ball around state s with radius ϵ : $B_p(s, \epsilon) := \{s' \mid \|s' - s\|_p \leq \epsilon\}$. We use a ϵ schedule during training, where ϵ is slowly increasing during each epoch t as ϵ_t .

Hyperparameters for Regular PPO training We use the optimal hyperparameters in [10] which were found using a grid search for vanilla PPO. We run 2048 simulation steps per iteration, and run policy optimization of 10 epochs with a minibatch size of 64 using Adam optimizer with learning rate 0.0004. The value network is also trained in 10 epochs per iteration with a minibatch size of 64, using Adam optimizer with learning rate 0.0003. Both networks are 3-layer MLPs with [64, 64] hidden neurons. The clipping value ϵ for PPO is 0.2. We clip rewards to $[-10, 10]$ and states to $[-10, 10]$. The discount factor γ for reward is 0.99 and the discount factor used in generalized advantage estimation (GAE) is 0.95. We found that in [10] the agent rewards are still improving when training finishes, thus in our experiments we run the agents longer for better convergence: we run Walker2d and Hopper 2×10^6 steps (976 iterations) and Humanoid 1×10^7 steps (4882 iterations) to ensure convergence.

Hyperparameter for SA-PPO training For SA-PPO, we use the same set of hyperparameters as in PPO. Note that the hyperparameters are tuned for PPO but not specifically for SA-PPO. The additional regularization parameter κ_{PPO} for the regularizer \mathcal{R}_{PPO} is chosen in $\{0.01, 0.03, 0.1, 0.3\}$. We linearly increase ϵ_t , the norm of ℓ_∞ perturbation on normalized states, from 0 to the target value (ϵ for evaluation, reported in Table 1) during the first 3/4 iterations, and keep $\epsilon_t = \epsilon$ for the reset iterations. The same ϵ schedule is used for both SGLD and convex relaxation training. For SGLD, we run 10 iterations with step size $\frac{\epsilon_t}{10}$ and set the temperature parameter $\beta = 1 \times 10^{-5}$. For convex relaxations, we use the efficient IBP+Backward scheme [72], and we use a training schedule similar to [77] by mixing the IBP bounds and backward mode perturbation analysis bounds.

G Additional details for SA-DDPG

Algorithm We present the SA-DDPG training algorithm in Algorithm 6. The main difference comparing to regular DDPG is the additional loss term $L_{SA}(\theta_\pi)$, which provides an upper bound on $\max_{s \in B(s_i)} \|\pi(s) - \pi(s_i)\|_2^2$. We define the perturbation set $B(s)$ to be a ℓ_p norm ball around s with

Algorithm 5 State-Adversarial Proximal Policy Optimization (SA-PPO)

Input: Number of iterations T , a ϵ schedule ϵ_t

- 1: Initialize actor network $\pi(a|s)$ and critic network $V(s)$ with parameter θ_π and θ_V ,
- 2: **for** $t = 1$ to T **do**
- 3: Run π_{θ_π} to collect a set of trajectories $\mathcal{D} = \{\tau_k\}$ containing $|\mathcal{D}|$ episodes, each τ_k is a trajectory contain $|\tau_k|$ samples, $\tau_k := \{(s_{k,i}, a_{k,i}, r_{k,i}, s_{k,i+1})\}, i \in [|\tau_k|]$
- 4: Compute cumulative reward $\hat{R}_{k,i}$ for each step i in every episode k using the trajectories and discount factor γ
- 5: Update Value function by minimizing the mean-square error:

$$\theta_V \leftarrow \arg \min_{\theta_V} \frac{1}{\sum_k |\tau_k|} \sum_{\tau_k \in \mathcal{D}} \sum_{i=0}^{|\tau_k|} (V(s_{k,i}) - \hat{R}_{k,i})^2$$

- 6: Estimate advantage $\hat{A}_{k,i}$ for each step i in every episode k using generalized advantage estimation (GAE) and value function $V_{\theta_V}(s)$
- 7: Define the robust policy regularizer:

$$L_{\text{SA}}(\theta_\pi) := \frac{1}{\sum_k |\tau_k|} \sum_{\tau_k \in \mathcal{D}} \sum_{i=0}^{|\tau_k|} \max_{\bar{s}_{k,i} \in B_p(s_{k,i}, \epsilon_t)} D_{\text{KL}}(\pi(a|s_{k,i}) \| \pi(a|\bar{s}_{k,i}))$$

- 8: Option 1: Solve $L_{\text{SA}}(\theta_\pi)$ using SGLD:
- 9: find $\hat{s}_{k,i} = \arg \max_{\bar{s}_{k,i} \in B_p(s_{k,i}, \epsilon_t)} \frac{1}{\sum_k |\tau_k|} \sum_{\tau_k \in \mathcal{D}} \sum_{i=0}^{|\tau_k|} D_{\text{KL}}(\pi(a|s_{k,i}) \| \pi(a|\bar{s}_{k,i}))$ using SGLD optimization
- 10: set $\bar{L}_{\text{SA}}(\theta_\pi) := \frac{1}{\sum_k |\tau_k|} \sum_{\tau_k \in \mathcal{D}} \sum_{i=0}^{|\tau_k|} D_{\text{KL}}(\pi(a|s_{k,i}) \| \pi(a|\hat{s}_{k,i}))$
- 11: Option 2: Solve $L_{\text{SA}}(\theta_\pi, \bar{s}_i)$ using convex relaxations:
- 12: $\bar{L}_{\text{SA}}(\theta_\pi) := \text{ConvexRelaxUB}(L_{\text{SA}}, \theta_\pi, \bar{s}_{k,i} \in B_p(s_{k,i}, \epsilon_t))$
- 13: Update the policy by minimizing the SA-PPO objective (the minimization is solved using ADAM):

$$\theta_\pi \leftarrow \arg \min_{\theta'_\pi} \frac{1}{\sum_k |\tau_k|} \sum_{\tau_k \in \mathcal{D}} \sum_{i=0}^{|\tau_k|} \min \left(r_{\theta'_\pi}(a_{k,i}|s_{k,i}) \hat{A}_{k,i}, g(r_{\theta'_\pi}(a_{k,i}|s_{k,i})) \hat{A}_{k,i} \right) + \kappa_{\text{PPO}} \bar{L}_{\text{SA}}(\theta'_\pi)$$

$$\text{where } r_{\theta'_\pi}(a_{k,i}|s_{k,i}) := \frac{\pi_{\theta'_\pi}(a_{k,i}|s_{k,i})}{\pi_{\theta_\pi}(a_{k,i}|s_{k,i})}, g(r) := \text{clip}(r_{\theta'_\pi}(a_{k,i}|s_{k,i}), 1 - \epsilon_{\text{clip}}, 1 + \epsilon_{\text{clip}})$$

- 14: **end for**

radius ϵ : $B_p(s, \epsilon) := \{s' \mid \|s' - s\|_p \leq \epsilon\}$. We use a ϵ schedule during training, where ϵ is slowly increasing during training as ϵ_t .

Algorithm 6 State-Adversarial Deep Deterministic Policy Gradient (SA-DDPG)

Initialize actor network $\pi(s)$ and critic network $Q(s, a)$ with parameter θ_π and θ_Q
 Initialize target network $\pi'(s)$ and critic network $Q'(s, a)$ with weights $\theta_{\pi'} \leftarrow \theta_\pi$ and $\theta_{Q'} \leftarrow \theta_Q$
 Initial replay buffer \mathcal{B}
for $t = 1$ to T **do**
 Initial a random process \mathcal{N} for action exploration
 Choose action $a_t \sim \pi(s_t) + \epsilon$, $\epsilon \sim \mathcal{N}$
 Observe reward r_t , next state s_{t+1} from environment
 Store transition $\{s_t, a_t, r_t, s_{t+1}\}$ into \mathcal{B}
 Sample a mini-batch of N samples $\{s_i, a_i, r_i, s'_i\}$ from \mathcal{B}
 $y_i \leftarrow r_i + \gamma Q'(s'_i, \pi'(s'_i))$ for all $i \in [N]$
 Update θ_Q by minimizing loss $L(\theta_Q) = \frac{1}{N} \sum_i (y_i - Q(s_i, a_i))^2$
 $L_{SA}(\theta_\pi, \bar{s}_i) := \frac{1}{N} \sum_i \max_{\bar{s}_i \in B_p(s_i, \epsilon_t)} \|\pi_{\theta_\pi}(s_i) - \pi_{\theta_\pi}(\bar{s}_i)\|_2$
 Option 1: Solve $L_{SA, \bar{s}_i}(\theta_\pi)$ using SGLD:
 find $\hat{s}_i = \arg \max_{\bar{s}_i \in B_p(s_i, \epsilon_t)} \sum_i \|\pi_{\theta_\pi}(s_i) - \pi_{\theta_\pi}(\bar{s}_i)\|_2$
 set $\bar{L}_{SA}(\theta_\pi) := \frac{1}{N} \sum_i \|\pi_{\theta_\pi}(s_i) - \pi_{\theta_\pi}(\hat{s}_i)\|_2$
 Option 2: Solve $L_{SA}(\theta_\pi, \bar{s}_i)$ using convex relaxations:
 $\bar{L}_{SA}(\theta_\pi) := \text{ConvexRelaxUB}(L_{SA}, \theta_\pi, \bar{s}_i \in B_p(s_i, \epsilon_t))$
 Update θ_π using deterministic policy gradient and gradient of $L_{SA}(\theta_\pi)$:
 $\nabla_{\theta_\pi} J(\theta_\pi) = \frac{1}{N} \sum_i [\nabla_a Q(s, a)|_{s=s_i, a=\pi(s_i)} \nabla_{\theta_\pi} \pi(s)|_{s=s_i} + \kappa_{DDPG} \nabla_{\theta_\pi} \bar{L}_{SA}(\theta_\pi)]$
 Update Target Network:
 $\theta_{Q'} \leftarrow \tau \theta_Q + (1 - \tau) \theta_{Q'}$
 $\theta_{\pi'} \leftarrow \tau \theta_\pi + (1 - \tau) \theta_{\pi'}$
end for

Hyperparameters for Regular DDPG training. Both actor and critic networks are 3-layer MLPs with [400, 300] hidden neurons. We run each environment for 2×10^6 steps. Actor network learning rate is 1×10^{-4} and critic network learning rate is 1×10^{-3} (except that for Hopper-v2 the learning rate is reduced to 1×10^{-4} due to the larger values of rewards); both networks are optimized using Adam optimizer. No reward scaling is used, and discount factor is set to 0.99. We use a replay buffer with a capacity of 1×10^6 items and we do not use prioritized replay buffer sampling. For the random process \mathcal{N} used for exploration, we use a Ornstein-Uhlenbeck process with $\theta = 0.15$ and $\sigma = 0.2$. The mixing parameter of current and target actor and critic networks is set to $\tau = 0.001$.

Hyperparameters for SA-DDPG training. SA-DDPG uses the same hyperparameters as in DDPG training. For the additional regularization parameter κ for $\pi(s)$, we choose $\kappa \in \{3.0, 10.0, 30.0, 100, 300\}$. We train the actor network without actor regularization for the first 1×10^6 steps, then increase ϵ from 0 to the target value in 5×10^5 steps, and then keep training at the target ϵ for 5×10^5 steps. The same ϵ schedule is used for both SGLD and convex relaxation. For SGLD, we run 5 iterations with step size $\frac{\epsilon_t}{5}$ and set the temperature parameter $\beta = 1 \times 10^{-5}$. For convex relaxations, we use the efficient IBP+Backward scheme [72], and a training schedule similar to [77] by mixing the IBP bounds and backward mode perturbation analysis bounds. The total number of training steps is thus 2×10^6 , which is the same as the regular DDPG training. The target ϵ values for each task is the same as ϵ listed in Table 2 for evaluation, except that for InvertedPendulum we set $\epsilon = 0.75$ during training. Note that we rescale ϵ by the standard deviations of each state variable. The standard deviations are calculated using data collected on baseline policy without adversaries.

H Additional details for SA-DQN

Algorithm We present the SA-DQN training algorithm in Algorithm 7. The main difference comparing to regular DQN is the additional hinge loss term \tilde{L} , which encourage the network not to change its output under perturbations on the state observation.

Algorithm 7 State-Adversarial Deep Q-Learning (SA-DQN)

- 1: Initialize current Q network $Q(s, a)$ with parameters θ .
- 2: Initialize target Q network $Q'(s, a)$ with parameters $\theta' \leftarrow \theta$.
- 3: Initial replay buffer \mathcal{B}
- 4: **for** $t = 1$ to T **do**
- 5: With probability ϵ_t select a random action at a_t , otherwise select $a_t = \arg \max_a Q_\theta(s_t, a; \theta)$
- 6: Execute action a_t in environment and observe reward r_t and state s_{t+1}
- 7: Store transition $\{s_t, a_t, r_t, s_{t+1}\}$ in \mathcal{B} .
- 8: Randomly sample a minibatch of N samples $\{s_i, a_i, r_i, s'_i\}$ from \mathcal{B} .
- 9: For all s_i , compute $a_i^* = \arg \max_a Q_\theta(s_i, a; \theta)$.
- 10: Set $y_i = r_i + \gamma \max_{a'} Q'_{\theta'}(s'_i, a'; \theta)$ for non-terminal s_i , and $y_i = r_i$ for terminal s_i .
- 11: Compute TD-loss for each transition: $\text{TD-}L(s_i, a_i, s'_i; \theta) = \text{Huber}(y_i - Q_\theta(s_i, a_i; \theta))$
- 12: Option 1: Use projected gradient descent (PGD)
- 13: Run PGD to solve: $\hat{s}_i = \arg \max_{\hat{s}_i \in B(s_i)} \max_{a_j \neq a_i^*} Q_\theta(\hat{s}_i, a_j; \theta) - Q_\theta(\hat{s}_i, a_i^*; \theta)$.
- 14: Compute hinge loss for each s_i :

$$\tilde{L}(s_i; \theta) = \max \left\{ \max_{\hat{s}_i \in B(s_i)} \max_{a_j \neq a_i^*} Q_\theta(\hat{s}_i, a_j; \theta) - Q_\theta(\hat{s}_i, a_i^*; \theta), -c \right\}$$
- 15: Option 2: Use convex relaxations of neural networks
- 16: For all s_i and all $a_j \neq a_i^*$, obtain upper bounds on $Q_\theta(s, a_j; \theta) - Q_\theta(s, a_i^*; \theta)$:

$$u_{a_i^*, a_j}(s_i; \theta) = \text{ConvexRelaxUB}(Q_\theta(s, a_j; \theta) - Q_\theta(s, a_i^*; \theta), \theta, s \in B(s_i))$$
- 17: Compute hinge loss for each s_i : $\tilde{L}(s_i; \theta) = \max \left\{ \max_{a_j \neq a_i^*} \{u_{a_i^*, a_j}(s_i)\}, -c \right\}$
- 18: Perform a gradient descent step to minimize $\frac{1}{N} \sum_i \text{TD-}L(s_i, a_i, s'_i; \theta) + \kappa_{\text{DQN}} \tilde{L}(s_i; \theta)$.
- 19: Update Target Network every M steps: $\theta' \leftarrow \theta$.
- 20: **end for**

Hyperparameters for Regular DQN training. For Atari games, the deep Q networks have 3 CNN layers followed by 2 fully connected layers. The first CNN layer has 32 channels, a kernel size of 8, and stride 4. The second CNN layer has 64 channels, a kernel size of 4, and stride 2. The third CNN layer has 64 channels, a kernel size of 3, and stride 1. The fully connected layers have 512 hidden neurons. For Atari games, we run each environment for 6×10^6 steps without framestack. For Acrobot, the deep Q network is a 3-layer MLP with [128, 128] hidden neurons and we run 6×10^5 steps. The learning rate is 1×10^{-3} for Acrobot, 1×10^{-5} for BankHeist, 2×10^{-5} for RoadRunner, and 6.25×10^{-5} for Pong and Freeway. For all environments, no reward scaling is used, and discount factor is set to 0.99. For all Atari environments, we use a replay buffer with a capacity of 2×10^5 and for Acrobot, the capacity is reduced to 2×10^4 . Prioritized replay buffer sampling is used with $\alpha = 0.5$ and β increased from 0.4 to 1 linearly in 6×10^5 for Acrobot and 4×10^6 steps for Atari games. A batch size of 32 is used and the target network is updated every 2000 steps. We use Huber loss in TD-loss.

Hyperparameters for SA-DQN training. SA-DQN uses the same network structure and hyperparameters as in DQN training, except that for Freewaay and BankHeist, we increase the schedule length of buffer's β to 6×10^6 . For the additional regularization parameter κ for robustness, we choose $\kappa \in \{0.005, 0.01, 0.02\}$. The total number of SA-DQN training steps in all environments are the same as those in DQN. For Pong and RoadRunner, we train the Q network without regularization for the first 1.5×10^6 steps, then increase ϵ from 0 to the target value in 2×10^6 steps, and then keep training at the target ϵ for 2.5×10^6 steps. For Freeway and BankHeist, this ϵ schedule starts

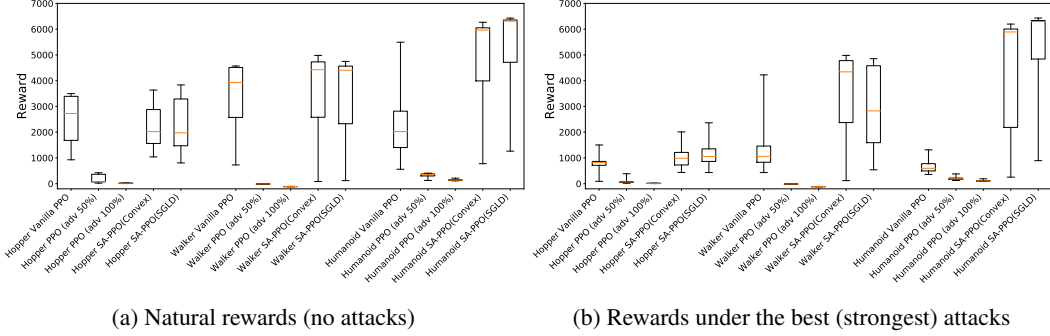


Figure 10: Box plots of natural rewards and rewards under the strongest (best) attacks for PPO, adversarially trained PPO and SA-PPO agents corresponding to the results presented in Table 1 (Table 1 only reports mean and standard deviation). Each box shows the distribution of accumulated rewards collected from 50 episodes of a single model. The red lines inside the boxes are median rewards, and the upper and lower sides of the boxes show 25% and 75% percentile rewards of 50 episodes. The line segments outside of the boxes show min or max rewards.

at 1×10^6 th step with a length of 4×10^6 steps. For Acrobot, this ϵ schedule starts at 2×10^4 th step with a length of 1×10^5 steps. For convex relaxations, we use the efficient IBP+Backward scheme [72], and we use a training schedule similar to [77] by mixing the IBP bounds and backward mode perturbation analysis bounds. The confidence constant c of hinge loss is 1 in Atari environments and is 0.01 in Acrobot.

I Additional Experimental Results

I.1 More results on SA-PPO

Box plots of rewards for SA-PPO models In Table 1, we report the mean and standard deviation of rewards for models under attack. However, since the distribution of accumulative rewards can be non-Gaussian, in this section we include box plots of rewards for each task in Figure 10. We can observe that the rewards (median, 25% and 75% percentiles) under the strongest attacks (Figure 10b) significantly improve.

Evaluation using multiple ϵ In Figure 11 we show the attack reward of PPO and SA-PPO models with different perturbation budget ϵ . We can see that the lowest attack rewards of SA-PPO models are higher than those of PPO under all ϵ values. Additionally, Robust Sarsa attacks are stronger comparing to other attacks. On vanilla PPO models, MAD attack is also competitive.

Convergence of PPO and SA-PPO agents Especially, we want to confirm that our significantly better performing Humanoid model is not just by chance. We train each environment using SA-PPO and PPO *at least 30 times*, and collect rewards during training. We plot the median, 25% and 75% percentile of all these runs in Figure 12 and here we report the moving average value of 10 consecutive episodes.

We can see that our SA-PPO models’ natural reward during training significantly and consistently outperforms PPO models in Humanoid. Since we also present the 25% and 75% percentile of the rewards among 30 models, we believe this improvement is not because of cherry-picking. For Hopper and Walker environments, SA-PPO achieves slightly lower but still quite competitive rewards; SA-PPO agents obtain significantly more robustness.

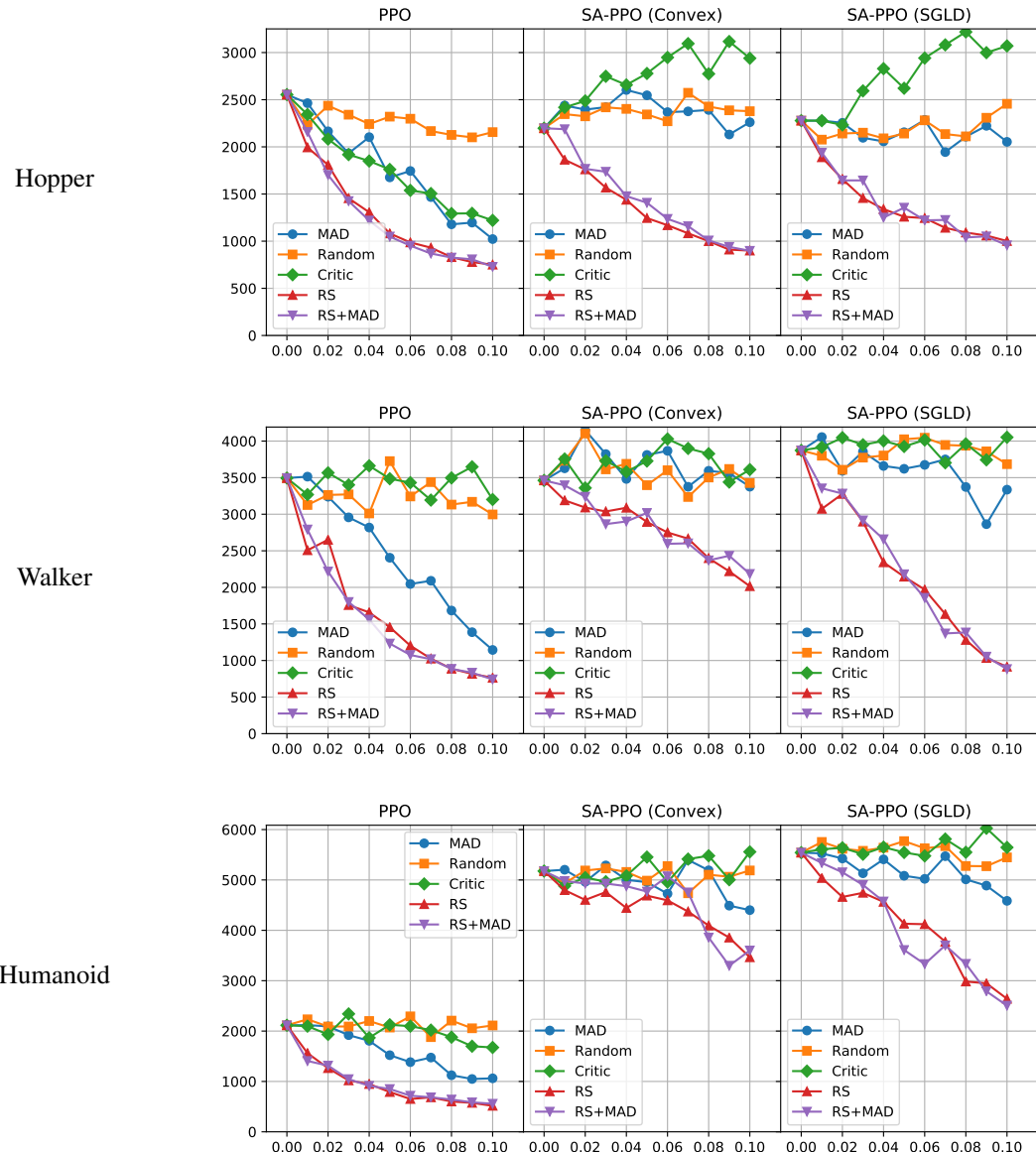


Figure 11: Attacking PPO agents under different ϵ values. Each data point reported in this figure is an average of 50 episodes.

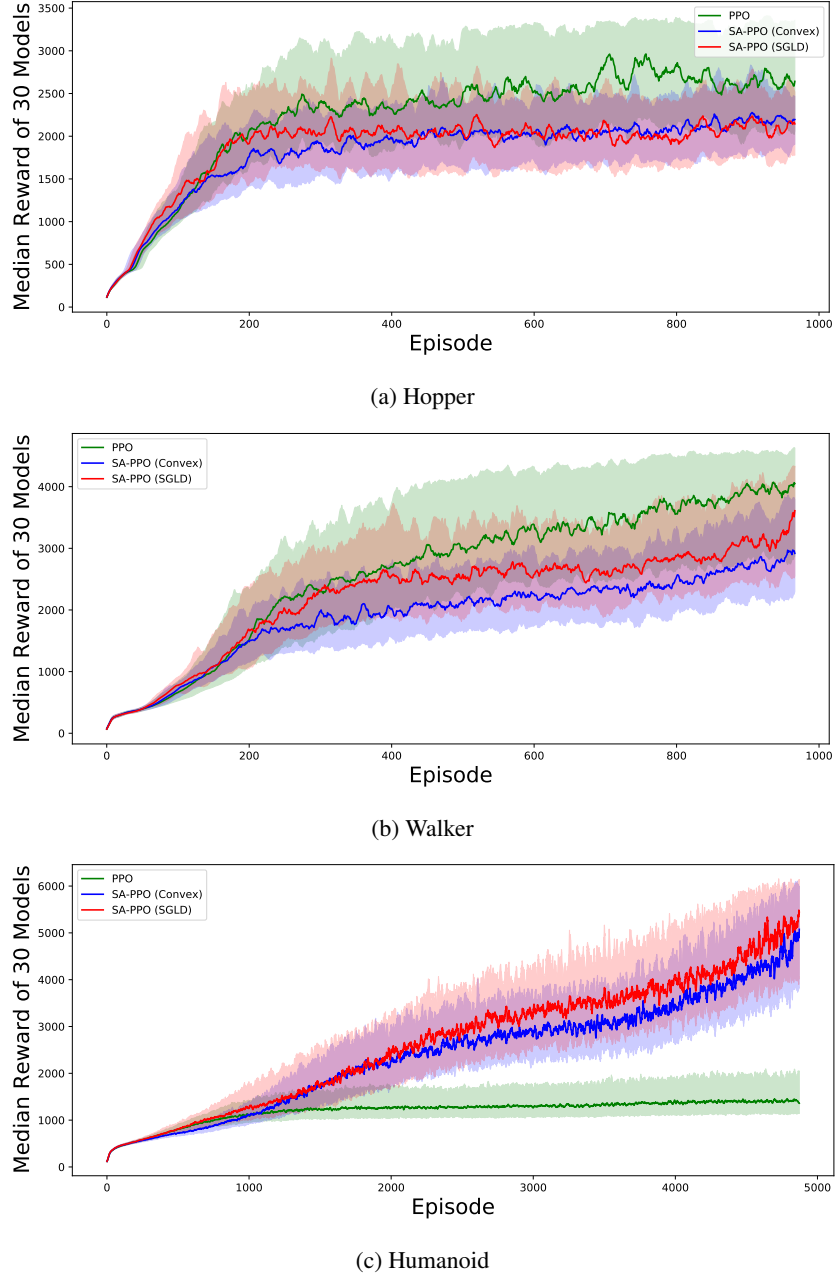


Figure 12: The median, 25% and 75% percentile episode reward of 30 PPO and 30 SA-PPO models during training. We report the moving average value of 10 consecutive episodes. The region of the shaded colors (light blue: SA-PPO solved with SGLD; light green: SA-PPO solved with convex relaxations; light red: vanilla PPO) represent the interval between 25% and 75% percentile rewards over the 30 different training runs, and the solid line is the median rewards over 30 runs.

I.2 More results on SA-DDPG

Full attack results In Table 7 we present attack rewards on all of our DDPG models. In the main text, we only report the strongest (lowest) attack rewards since the lowest reward determines the true model robustness.

Table 6: Comparison between Smoothed and Non-smoothed policies on SA-DDPG (Convex) models in Table 2. We report mean reward \pm standard deviation over 50 attack episodes.

Env.	ℓ_∞ norm perturbation budget ϵ	Smoothed Natural Reward	Non-smoothed Natural Reward	Smoothed Best Attack Reward	Non-smoothed Best Attack Reward
Ant	0.2	2129.70 \pm 60.54	2111.22 \pm 158.88	1963.91 \pm 56.19	1958.79 \pm 105.24
Hopper	0.075	3348.96 \pm 516.18	3496.25 \pm 30.84	1555.24 \pm 953.33	1603.90 \pm 589.46
InvertedPendulum	0.5	1000.00 \pm 0.00	1000.00 \pm 0.00	800.98 \pm 329.25	877.86 \pm 279.33
Reacher	1.5	-5.43 \pm 2.26	-5.22 \pm 2.12	-12.51 \pm 4.74	-13.86 \pm 3.82
Walker2d	0.15	3379.16 \pm 1433.54	4234.60 \pm 853.86	2079.65 \pm 1069.95	1944.77 \pm 1143.25

Adding noise to DDPG and SA-DDPG In Section 3.3, our theory requires to use a smoothed policy $\bar{\pi}$ with added Gaussian noise σ . In Section 4, we have reported SA-DDPG performance without adding σ . In this section, we present results with noise $\sigma \sim \mathcal{N}(0, 0.1)$ for smoothed DDPG policies. Table 6 shows the results. We can observe that clean performance of the smoothed DDPG policies slightly drops while the robustness (reward under attacks) can be slightly better than the non-smoothed policies in most settings.

I.3 Robustness Certificates

We report robustness certificates for SA-DQN in Table 3. As discussed in section E, for DQN we can guarantee that an action does not change under bounded adversarial noise. In Table 3, the ‘‘Action Cert. Rate’’ is the ratio of actions that does not change under any ℓ_∞ norm bounded noise. In some settings, we find that 100% of the actions are guaranteed to be unchanged (e.g., the Pong environment in Table 3). In that case, we can in fact also certify that the accumulated reward is not changed given the specific initial conditions for testing.

In SA-DDPG, we can obtain robustness certificates that give bounds on actions in the presence of bounded perturbation on state inputs. Given an input state s , we use convex relaxations of neural networks to obtain the upper and lower bounds for each action: $l_i(s) \leq \pi_i(\hat{s}) \leq u_i(s), \forall \hat{s} \in B(s)$. We consider the following certificates on $\pi(s)$: the average output range $\frac{\|u(s) - l(s)\|_1}{|\mathcal{A}|}$ which reflect the tightness of bounds, and the ℓ_2 distance. Note that bounds on other ℓ_p norms can also be computed given $l_i(s)$ and $u_i(s)$. Since the action space is normalized within $[-1, 1]$, the worst case output range is 2. We report both certificates for all five environments in Table 8. DDPG without our robust regularizer usually cannot obtain non-vacuous certificates (range is close to 2). SA-DDPG can provide robustness certificates (bounded inputs guarantee bounded outputs). We include some discussions on these certificates in Section E.

For SA-PPO, since the action follows a Gaussian policy, we can upper bound its KL-divergence under state perturbations. The results are shown in Table 9.

Environment		Ant	Hopper	Inverted Pendulum	Reacher	Walker2d
ϵ		0.2	0.075	0.5	1.5	0.15
State Space		111	11	4	11	17
Vanilla DDPG	Natural Reward	1633 \pm 631	3180 \pm 390	1000 \pm 0	-4.4 \pm 1.6	2247 \pm 1177
	Critic Attack	337 \pm 299	2112 \pm 903	1000 \pm 0	-25.1 \pm 4.9	1193 \pm 1252
	Random Attack	1277 \pm 704	2903 \pm 736	1000 \pm 0	-8.35 \pm 2.43	1764 \pm 1152
	MAD Attack	199 \pm 225	1396 \pm 809	315 \pm 243	-27.8 \pm 5.83	1557 \pm 1372
	RS Attack	368 \pm 346	704 \pm 228	1000 \pm 0	-17.1 \pm 3.76	711 \pm 663
	RS+MAD	257 \pm 247	783 \pm 610	285 \pm 232	-27.94 \pm 5.47	1057 \pm 1028
	Best Attack	199	704	285	-27.85	711
DDPG with adv. training (50% steps) Pattanaik et al. [43]	Natural Reward	715 \pm 265	3010 \pm 460	1000 \pm 0	-4.79 \pm 1.49	1029 \pm 316
	Critic Attack	393 \pm 290	1396 \pm 1001	336 \pm 280	-28.95 \pm 5.1	103 \pm 118
	Random Attack	665 \pm 295	2920 \pm 624	966 \pm 146	-8.86 \pm 2.4	703 \pm 548
	MAD Attack	304 \pm 284	1872 \pm 1338	106 \pm 81	-32.13 \pm 6.56	172 \pm 165
	RS Attack	160 \pm 301	13.8 \pm 3.4	154 \pm 49	-16.9 \pm 2.6	261 \pm 371
	RS+MAD	333 \pm 247	14.7 \pm 3.6	199 \pm 209	-32.4 \pm 6.2	111 \pm 91
	Best Attack	160	13.8	106	-32.4	103
DDPG with adv. training (100% steps) Pattanaik et al. [43]	Natural Reward	63.8 \pm 79	2680 \pm 810	1000 \pm 0	-5.97 \pm 2.39	1242 \pm 254
	Critic Attack	1.2 \pm 32.6	2562 \pm 797	983 \pm 93	-28.6 \pm 4.6	118 \pm 148
	Random Attack	81 \pm 79.7	2800 \pm 437	1000 \pm 0	-10.2 \pm 2.7	957 \pm 619
	MAD Attack	-14.9 \pm 28	2731 \pm 679	410 \pm 302	-31.15 \pm 4.7	128 \pm 191
	RS Attack	-65 \pm 91.6	1778 \pm 577	1000 \pm 0	-21.3 \pm 4	41.7 \pm 20.1
	RS+MAD	-57.5 \pm 71	413 \pm 552	345 \pm 290	-31.3 \pm 4.6	115 \pm 157
	Best Attack	-57.5	413	345	-31.3	41.7
SA-DDPG solved by SGLD	Natural Reward	1503 \pm 502	3035 \pm 4.34	1000 \pm 0	-5.2 \pm 1.64	2760 \pm 1563
	Critic Attack	1294 \pm 540	3069 \pm 69.5	1000 \pm 0	-11.7 \pm 5.13	817 \pm 747
	Random Attack	1519 \pm 405	3026 \pm 11.5	1000 \pm 0	-11.7 \pm 4.86	2923 \pm 1443
	MAD Attack	1251 \pm 543	2933 \pm 287	1000 \pm 0	-11.9 \pm 5.23	2304 \pm 1729
	RS Attack	1371 \pm 351	2564 \pm 562	1000 \pm 0	-11.2 \pm 5.16	838 \pm 1275
	RS+MAD	1289 \pm 423	2537 \pm 745	1000 \pm 0	-11.87 \pm 5.21	1365 \pm 682
	Best Attack	1251	2537	1000	-11.9	817
SA-DDPG solved by convex relaxations	Natural Reward	2111 \pm 159	3496 \pm 30.8	1000 \pm 0	-5.222 \pm 2.12	4234 \pm 854
	Critic Attack	1959 \pm 105	3162 \pm 829	1000 \pm 0	-12.7 \pm 4.5	1945 \pm 1143
	Random Attack	2051 \pm 377	3490 \pm 44	1000 \pm 0	-9.77 \pm 4.75	3659 \pm 1279
	MAD Attack	2070 \pm 167	3403 \pm 342	1000 \pm 0	-12.8 \pm 4.5	2900 \pm 1511
	RS Attack	2011 \pm 108	1722 \pm 599	1000 \pm 0	-13.6 \pm 3.64	2207 \pm 1266
	RS+MAD	1995 \pm 301	1604 \pm 589	878 \pm 279	-13.9 \pm 3.8	3199 \pm 1482
	Best Attack	1959	1722	878	-13.9	1945

Table 7: Rewards on 5 Mujoco environments using policies trained by DDPG and SA-DDPG. Natural reward is the reward in clean environment without adversarial attacks. The “Best Attack” rows report the lowest reward over all four attacks (representing the strongest attack), and this lowest reward is used for robustness evaluation.

Table 8: Robustness certificates on bounded action changes under bounded state perturbations for DDPG models. Results are averaged over 50 episodes. A smaller number is better. A vanilla DDPG model typically cannot provide non-vacuous robustness guarantees.

Model		Ant	Hopper	InvertedPendulum	Reacher	Walker2d
Certificates (ℓ_2 upper bound)	SA-DDPG (Convex)	0.129	0.285	0.040	0.207	0.563
	DDPG (vanilla)	4.169	2.453	1.033	1.493	4.504
Certificates (ℓ_1 upper bound)	SA-DDPG (Convex)	0.328	0.404	0.040	0.290	1.095
	DDPG (vanilla)	11.625	3.985	1.033	2.111	10.875
Certificates (ℓ_∞ upper bound)	SA-DDPG (Convex)	0.076	0.243	0.040	0.162	0.414
	DDPG (vanilla)	1.813	1.746	1.033	1.075	1.999
Certificates (Range)	SA-DDPG (Convex)	0.041	0.135	0.040	0.145	0.182
	DDPG (vanilla)	1.453	1.328	1.033	1.055	1.812

Table 9: Upper bound on KL-divergence $D_{KL}(\pi(a|s) \parallel \pi(a|\hat{s}))$ for three PPO environments. A smaller number is better. Surprisingly, a vanilla trained Hopper and Walker2d models already have relatively smaller upper bound on KL-divergence (but still larger than SA-PPO). However, for Humanoid our SA-PPO can reduce this upper bound significantly.

Model		Hopper	Walker2d	Humanoid
Certificates (KL upper bound)	SA-PPO (Convex)	5.0013	0.8201	2.0414
	PPO (vanilla)	8.1455	1.4210	403.05